

---

# WHAT MATTERS IN DEEP LEARNING FOR TIME SERIES FORECASTING?

---

Valentina Moretti<sup>1</sup>, Andrea Cini<sup>3,1\*</sup>, Ivan Marisca<sup>1</sup>, Cesare Alippi<sup>1,2</sup>

<sup>1</sup>IDSIA, Università della Svizzera italiana, Lugano, Switzerland

<sup>2</sup>Politecnico di Milano, Milan, Italy

<sup>3</sup>Swiss National Science Foundation Postdoctoral Fellow

{valentina.moretti, andrea.cini, ivan.marisca, cesare.alippi}@usi.ch

## ABSTRACT

Deep learning models have grown increasingly popular in time series applications. However, the large quantity of newly proposed architectures, together with often contradictory empirical results, makes it difficult to assess which components contribute significantly to final performance. We aim to make sense of the current design space of deep learning architectures for time series forecasting by discussing the design dimensions and trade-offs that can explain, often unexpected, observed results. This paper discusses the necessity of grounding model design on principles for forecasting groups of time series and how such principles can be applied to current models. In particular, we assess how concepts such as locality and globality apply to recent forecasting architectures. We show that accounting for these aspects can be more relevant for achieving accurate results than adopting specific sequence modeling layers and that simple, well-designed forecasting architectures can often match the state of the art. We discuss how overlooked implementation details in existing architectures (1) fundamentally change the class of the resulting forecasting method and (2) drastically affect the observed empirical results. Our results call for rethinking current faulty benchmarking practices and the need to focus on the foundational aspects of the forecasting problem when designing architectures. As a step in this direction, we propose an *auxiliary forecasting model card*, whose fields serve to characterize existing and new forecasting architectures based on key design choices.

**Keywords** time series forecasting · deep learning for time series · time series benchmarks

## 1 Introduction

Novel sequence modeling architectures are consistently improving the state-of-the-art in many applications [Gu et al., 2022, Gu and Dao, 2024, Beck et al., 2024], such as natural language processing. However, results in time series forecasting offer a much more uncertain way ahead, with recent work questioning the effectiveness of modern deep learning approaches [Toner and Darlow, 2024, Zeng et al., 2023, Tan et al., 2024]. The result is that current research is seemingly stuck in a loop of positive results being quickly dismissed by new evidence that questions our understanding of the components that contribute to obtaining accurate forecasts [Shao et al., 2024]. Recent works propose several architectures, e.g., based on attention [Zhou et al., 2021, Wu et al., 2021, Nie et al., 2023, Liu et al., 2023b, Zhang and Yan, 2023, Liu et al., 2022a], and assess their performance against state-of-the-art methods on common benchmarks. Most of these architectures are obtained by stacking and combining different components and operators and involve many—often hidden—implementation choices (e.g., parameter sharing and local parameters). However, the impact of such design choices on the resulting model and its performance is often overlooked. As an example, in recent works, a collection of synchronous time series is often considered as a single multivariate signal. This approach can lead to misconceptions and results that are difficult to interpret. Starting from this consideration, recent architectures stemming from Nie et al. [2023] rely on what has been called *channel-independence*, i.e., on processing each channel of a time series independently from others while sharing the same parameters. This approach has—somewhat surprisingly—led to

---

\*Work done while at the University of Oxford.

superior results when compared to standard multivariate models. However, when these channels correspond to different univariate and homogeneous time series (as is often the case in commonly used benchmarks), “channel-independence” corresponds to adopting the framework of global models, which is well understood in time series analysis [Benidis et al., 2022, Salinas et al., 2020, Januschowski et al., 2020, Montero-Manso and Hyndman, 2021]. While this might sound simply an issue of naming conventions, it can provide clear explanations for observed results [Montero-Manso and Hyndman, 2021] and motivate the development of architectures grounded in these principles [Wang et al., 2019, Smyl, 2020]. For example, there is a large body of literature on methods that account for dependencies among synchronous time series while keeping (part of) the model global [Cini et al., 2023, Sen et al., 2019]. As an additional example, other works have recently observed that applying attention among channels can improve performance [Liu et al., 2023b, Zhang and Yan, 2023]. However, if we consider the different channels as a collection of correlated time series, similar attention operators have been routinely used in spatiotemporal forecasting models [Ma et al., 2019, Grigsby et al., 2021, Marasca et al., 2022, Liu et al., 2023a]. These examples highlight how ignoring established principles for forecasting groups of time series can harm the effectiveness of our benchmarking practices. Indeed, overlooked design choices can, as we will show, lead to empirical results that are difficult to interpret and might mislead the designer. Moreover, as we discuss throughout the paper, those mentioned are only a selection of the issues that contribute to the current situation.

In this paper, we investigate how current benchmarking practices have shaped the current state of the field. We complement our analysis with an extensive empirical evaluation to assess whether commonly used benchmarks and evaluation practices accurately identify the factors contributing to reported performance gains. To pinpoint the specific sources of inconsistencies often observed in benchmarking results, we focus on four key design dimensions that significantly affect model performance. In particular, building on well-established principles for forecasting collections of time series, we structure our analysis around the following four dimensions: **D1. model configuration**, i.e., selecting the model family (e.g., local, global, or hybrid); **D2. preprocessing and exogenous variables**, i.e., selecting exogenous variables and setting up preprocessing and postprocessing operations; **D3. temporal processing**, i.e., accounting for temporal (i.e., intra-series) dependencies; **D4. spatial processing**, i.e., accounting for spatial (i.e., inter-series) dependencies. While some of these dimensions are not always orthogonal (e.g., space and time contributions can be processed in an integrated way), we believe that analyzing how these different aspects concur to characterize a model family is the key to understanding recent results. We show that the current approach to benchmarking forecasting architectures does not account for how key design choices affect performance, resulting in performance differences instead being attributed to the wrong components. The relevance of this finding is highlighted by our results, which show that simple architectures, such as multilayer perceptrons (MLPs), can surprisingly match state-of-the-art performance and that removing the core components introduced by state-of-the-art architectures can lead to a general performance improvement. We argue that, to assess meaningful improvements to the state of the art, any comparison must ensure that design choices in any of these dimensions do not interfere with the evaluation of the proposed component. In this context, our contributions are as follows.

- We analyze the current state of deep learning for time series forecasting by relying on principles to forecast groups of time series to make sense of often contradictory empirical results.
- We identify several critical issues in modern benchmarking practices that have led the community to misleading and seemingly contradictory conclusions.
- We empirically assess the impact of overlooked design choices and implementation details in existing state-of-the-art architectures, and show that they explain a significant portion of the observed performance improvements.
- We show that a streamlined architecture built on well-understood design principles can match the performance of the state-of-the-art.
- To move forward, we introduce an *auxiliary forecasting model card* template—complementary to existing generic model cards [Mitchell et al., 2019]—that can be used to characterize existing and new forecasting architectures.

The current trends in the field have led to a focus on finding a one-size-fits-all architecture with state-of-the-art performance in benchmarks. This prompted the adoption of increasingly more complex architectures that combine many poorly understood components. As we show, the problem has been exacerbated by recent benchmarking practices, which have been ineffective in comparing different architectures and in attributing performance gains to the components being introduced. By exposing these limitations and raising concerns about recent reported progress in the field, our work aims to stimulate discussion on our approach to conducting machine learning research for time series forecasting. We believe that having this discussion is an important step for the maturity of the field and to ensure future progress.

## 2 Related work and context

The history of neural networks in forecasting applications is long, and has often been characterized by skepticism [Zhang et al., 1998]. However, the forecasting community is reaching consensus on the effectiveness of deep learning methods in settings where a single neural network can be trained on (large) collections of related time series [Hewamalage et al., 2021, Benidis et al., 2022]. Models based on this approach have been called *global* in contrast with *local* models, which are instead trained separately on each time series [Montero-Manso and Hyndman, 2021, Januschowski et al., 2020, Benidis et al., 2022]. Global models and hybrid global-local variants thereof have won forecasting competitions [Smyl, 2020] and been adopted by the industry [Salinas et al., 2020, Kunz et al., 2023]. With the increase in popularity of new sequence modeling architectures [Vaswani et al., 2017, Gu et al., 2022, Gu and Dao, 2024, Orvieto et al., 2023], the machine learning community has started investigating how to adapt such architectures to the forecasting problem. In particular, the Informer [Zhou et al., 2021] architecture is among the first of a line of works aiming at tailoring Transformers [Vaswani et al., 2017] to long-range time series forecasting. Together with the architecture, Zhou et al. [2021] also introduced a popular benchmark where collections of time series are considered as a single multivariate sequence. However, conflating the problem of forecasting any group of time series into forecasting a single multivariate sequence, as we will see, can be problematic and lead to unclear designs (Sec. 4.1). Several subsequent works followed the same approach [Wu et al., 2021, Liu et al., 2022a, Wu et al., 2023, Liu et al., 2022b, Zhou et al., 2022]. Later, Zeng et al. [2023] and Toner and Darlow [2024] showed that most of these architectures can be outperformed in such benchmarks by simple linear models. In parallel, Nie et al. [2023] showed that—in the same settings—superior results could be achieved by processing each channel independently with shared parameters. For many of these benchmarks, this essentially corresponds to the global approach; indeed, a large part of the associated datasets consists of collections of related time series, even though, as already mentioned, they have often been treated as a single multivariate sequence. Follow-up works [Liu et al., 2023b, Zhang and Yan, 2023] reintroduced *spatial* components to model dependencies across multiple time series while keeping the core of the model global. Moreover, the focus on chasing state-of-the-art performance on benchmarks has led to designing increasingly complex architectures, often by stacking multiple components whose effectiveness often relies on hidden implementation details. As a result, it has become increasingly difficult to identify which elements truly drive performance.

The need to improve empirical research is a pressing issue in machine learning at large [Herrmann et al., 2024] and, in the context of time series forecasting, has motivated researchers to focus on developing new benchmarks and evaluation pipelines for forecasting [Shao et al., 2024, Wang et al., 2024b, Qiu et al., 2024]. Notably, [Brigato et al., 2025] shows that hyperparameter tuning and experimental details—such as the exclusion of specific datasets, prediction horizons, or baseline models—can drastically affect reported performance. In contrast, our work addresses a complementary but distinct issue. Rather than focusing on the impact of hyperparameter tuning or experimental selection and limitations in the datasets, we aim to assess whether the performance gains reported for recently proposed methods stem from the introduction of specific architectural operators or instead arise from other implementation details and design choices.

This motivates us to investigate whether current benchmarking practices are focusing on *what really matters* in deep learning for time series forecasting. Similar analysis has been pivotal in other areas of machine learning, such as reinforcement learning [Raichuk et al., 2021], and in the context of graph neural networks (GNNs) [Errica et al., 2020, Dwivedi et al., 2023, Bechler-Speicher et al., 2025].

## 3 Preliminaries

### 3.1 Problem setting

We consider a collection of  $N$  time series  $\mathcal{D} = \{\mathbf{x}_{0:L_1}^1, \dots, \mathbf{x}_{0:L_N}^N\}$ , where  $\mathbf{x}_{0:L_i}^i \in \mathbb{R}^{L_i \times d_x}$  denotes the sequence of  $L_i$   $d_x$ -dimensional observations associated with the  $i$ -th time series. Time series in the set can come from different domains and be generated by different stochastic processes. A binary mask,  $\mathbf{m}_{0:L_i}^i \in \{0, 1\}^{L_i \times d_x}$ , may be introduced to model missing or invalid observations, due to either acquisition errors, faults, or missing channels in the case of heterogeneous time series. When present, exogenous variables (e.g., time encoding, calendar features, weather conditions) are denoted as  $\mathbf{u}_{0:L_i}^i \in \mathbb{R}^{L_i \times d_u}$  and assumed to be available also when the corresponding observation is missing. If time series are synchronous, we use capital letters to denote values across the collection, e.g.,  $\mathbf{X}_t \in \mathbb{R}^{N \times d_x}$  refers to the stacked observations at time step  $t$ . Time series in the collection might be *correlated* (in a broad sense), i.e., uncertainty on future values of each time series might be reduced by taking into account observations from other time series.

**Forecasting groups of time series** We consider the problem of multi-step ahead time series forecasting, i.e., the problem of predicting the next  $H \geq 1$  observations  $\mathbf{x}_{t:t+H}^i$  for the  $i$ -th time series, given a window  $W \geq 1$  of past observations  $\mathbf{x}_{t-W:t}^i$  from the same time series. As the stochastic process generating data  $p^i$  is unknown, the objective

is to approximate it with a model  $p_{\theta}$  with learnable parameters  $\theta$  such that

$$p_{\theta}(\mathbf{x}_{t:t+H}^i \mid \mathbf{x}_{t-W:t}^i, \mathbf{u}_{t-W:t}^i, \mathbf{u}_{t:t+H}^i) \approx p^i(\mathbf{x}_{t:t+H}^i \mid \mathbf{x}_{<t}^i, \mathbf{u}_{<t}^i, \mathbf{u}_{t:t+H}^i) \quad \forall i = 1, \dots, N \quad (1)$$

where  $\mathbf{x}_{<t}^i$  denotes all past observations of the  $i$ -th series preceding timestep  $t$ . We focus on the problem of obtaining *point forecasts*  $\hat{\mathbf{x}}_{t:t+H}$  of, e.g., the expected value such as  $\hat{\mathbf{x}}_{t:t+H}^i \approx \mathbb{E}_p[\mathbf{x}_{t:t+H}^i]$  by using a parametric model  $\mathcal{F}(\cdot; \theta)$ . Predictions are obtained by fitting parameters  $\theta$  of the chosen model family. As we will discuss in Sec. 4.1, we say that a model is *global* if its parameters are shared across all the time series. In such a case, the model is trained on the entire set of time series. Conversely, a model is *local* if its parameters are specific to a single time series. If relying on local models, forecasting a collection of time series results in fitting a separate model for each sequence in the set. Choosing between a local and global approach (or a hybrid thereof) depends on the task at hand, data availability, and model complexity. As mentioned in Sec. 1, due to advantages in sample efficiency, global models are a particularly appealing choice when relying on deep learning architectures [Hewamalage et al., 2021, Benidis et al., 2022]. Additionally, global models can be employed inductively, e.g., in a cold start scenario, whereas local models are transductive. We will expand this discussion in Sec. 4.1.

### 3.2 Baselines

Through the paper, we assess the impact of different design choices with respect to a set of recent state-of-the-art architectures for long-range time series forecasting, which we compare against simpler, streamlined baselines. We consider representative models that have shaped the development of recent time series forecasting methods and that demonstrate competitive performance on benchmarks. We include: 1. **PatchTST** [Nie et al., 2023], the widely used architecture that—as already mentioned—introduced “channel independence” and patching-based Transformer layers. In particular, PatchTST relies on splitting the input into fixed-size patches before applying attention; 2. **DLinear** [Zeng et al., 2023], which combines a linear model with a time series decomposition step; 3. **TimeMixer** [Wang et al., 2024a], which uses MLPs to process the input at different resolutions; 4. **Linear**, a linear autoregressive model trained with  $L2$  regularization and ordinary least squares (OLS), following Toner and Darlow [2024], implemented in both its global and local variants. We also consider models that incorporate spatial processing: 5. **iTransformer** [Liu et al., 2023b], which processes the temporal dynamics with a feedforward layer and then uses standard attention among channels; 6. **ModernTCN** [Donghao and Xue, 2024] which employs convolutional layers for spatio-temporal representation; 7. **Crossformer** [Zhang and Yan, 2023], which uses patching and spatiotemporal attention operators to model dependencies among different channels of the input time series. To ensure a fair comparison, we evaluate all the models in the same benchmarking setup, under unified settings, and with access to the same exogenous variables. We rely on the available open-source implementations of each approach and adapt them to our evaluation procedure and standardized inputs. The code for all the experiments, based on the Torch Spatiotemporal library [Cini and Marisca, 2022], will be open-sourced upon publication. For details on each baseline, we refer readers to App. A.

**Reference architectures** In our experiments, we compare state-of-the-art models against a reference streamlined architecture specifically designed to assess the impact of different design choices w.r.t. the target design dimensions. Note that the purpose here is not to propose a new architecture to challenge the state of the art. Conversely, reference architectures provide baselines, introduced to facilitate a fair and consistent comparison and to gauge the impact of different design choices more directly. For the temporal module, we consider several alternatives: an MLP with residual connections, a temporal convolutional network (TCN) with causal dilated filters [Bai et al., 2018], a gated recurrent neural network (RNN) [Chung et al., 2014], a stack of Transform layers [Vaswani et al., 2017], and pyramidal attention operators akin to the Pyraformer architecture [Liu et al., 2022a]. In the tables, we denote these reference models as **MLP**, **TCN**, **RNN**, **Transf.**, **Pyraf.**, respectively. For the TCN, RNN and attention-based models, we use a 1- $D$  convolutional layer with a large stride as an additional preprocessing step to implement an operator akin to patching [Nie et al., 2023] and facilitate the processing at the subsequent layers. For the spatial module, we use a simple spatial attention layer (denoted as **sp. attn.**). For additional implementation details, please refer to App. B.

### 3.3 Benchmarks

As a benchmark, we use four real-world datasets from different domains that are widely used in the context of long-range time series forecasting [Wang et al., 2024a, Zhang and Yan, 2023, Liu et al., 2023b, Zeng et al., 2023, Nie et al., 2023]. In particular: **Electricity** collects hourly electricity usage for 321 customers [Wu et al., 2021]; **Weather** includes 21 meteorological variables collected every 10 minutes from Germany [Wu et al., 2021]; **Traffic** contains hourly road occupancy data collected from various 862 sensors on San Francisco’s highways [Wu et al., 2021]; **Solar** contains 10-minute records of solar power generation from 137 photovoltaic plants [Lai et al., 2018]. The extensive use of these datasets in prior studies makes them relevant for the present work. We use a 70%/10%/20% split for the training, validation, and testing, following previous works [Wang et al., 2024a]. Metrics are reported on scaled data for

consistency with published benchmarks. All the numerical results are averaged over three independent runs. We use a window size of 96 for all experiments in the main body of the paper, while in Tab. 3 we use a longer window size of 336 (except for Solar). For further details, refer to App. C.

## 4 What Matters in Deep Learning for Time Series Forecasting?

In this section, we go through four key design dimensions that characterize forecasting architectures and have a significant impact on overall performance. For each design dimension, we assess how different choices have contributed to making the current progress in the field uncertain, leading to often unexpected empirical results.

**D1. Model configuration** This refers to the type of forecasting model being employed. We distinguish between local models (each trained on individual time series), global models (trained on multiple series jointly with the same shared weights), and hybrid approaches that combine elements of both paradigms.

**D2. Preprocessing and exogenous variables** This dimension refers to the transformations applied to the data either before or after being used as input to a predictor, and to the exogenous variables used as additional inputs to the forecasting architecture.

**D3. Temporal processing** Temporal processing refers to the operators used to model temporal dependencies within an architecture.

**D4. Spatial processing** This dimension involves mechanisms used to model inter-series dependencies when multiple time series are available as inputs.

We do not aim to provide an exhaustive discussion of each dimension. Instead, we focus on how they have been addressed in recent research and on their role in explaining why current benchmarking practices struggle to effectively compare different architectures and attribute performance improvements. We identify that the main issues arise from how certain design choices have been incorporated into existing architectures without assessing their impact on performance. For the analysis, we selected widely used datasets and baselines that cover several core aspects of current machine learning for time series forecasting research.

### 4.1 Design dimension 1: Model configuration

As previously discussed, the model configuration—global, local, or hybrid—is a fundamental aspect in model design, since it radically changes the type of model being used. Yet, this aspect is often left unspecified or motivated as an implementation detail. However, choosing between a local, global, or hybrid approach has several implications that should be properly discussed [Montero-Manso and Hyndman, 2021, Januschowski et al., 2020, Salinas et al., 2020]. For instance, it is often common to model any collection of synchronous time series as a single highly-dimensional multivariate time series and hence consider models such as

$$\widehat{\mathbf{X}}_{t:t+H} = \mathcal{F}(\mathbf{X}_{t-W:t}, \dots; \boldsymbol{\theta}). \quad (2)$$

However, this approach can scale poorly with the input’s dimensionality. Indeed, in practice, several recent works (e.g., Nie et al. [2023], Liu et al. [2023b]) have observed that processing each channel independently with the same parameters empirically yields better performance. As already mentioned, this is equivalent to adopting the well-known global approach, i.e., to processing related time series as

$$\widehat{\mathbf{x}}_{t:t+H}^i = \mathcal{F}(\mathbf{x}_{t-W:t}^i, \dots; \boldsymbol{\theta}) \quad \forall i = 1, \dots, N. \quad (3)$$

Moreover—although not always explicitly stated—several architectures, e.g., [Wang et al., 2024a, Zhang and Yan, 2023, Donghao and Xue, 2024], adopt the approach in Eq. 3, but introduce some time series specific parameters  $\boldsymbol{\phi}^i$ , resulting in models

$$\widehat{\mathbf{x}}_{t:t+H}^i = \mathcal{F}(\mathbf{x}_{t-W:t}^i, \dots; \boldsymbol{\theta}, \boldsymbol{\phi}^i) \quad \forall i = 1, \dots, N. \quad (4)$$

which effectively consist of hybrid global-local models [Smyl, 2020, Cini et al., 2023, Benidis et al., 2022]. The design choices that lead to models as in Eq. 4 are often dealt with as implementation details. For instance, Wang et al. [2024a]

Table 1: Comparison (MSE) of models with local embeddings for a forecasting horizon of 96. Best average results are in **bold**.

D	Model	Hybrid	Global
Electr.	Transf.	<b>0.136<sub>±.000</sub></b>	0.151 <sub>±.000</sub>
	Crossformer	<b>0.141<sub>±.001</sub></b>	0.146 <sub>±.003</sub>
	TimeMixer	<b>0.151<sub>±.000</sub></b>	0.180 <sub>±.001</sub>
	iTransformer	<b>0.139<sub>±.000</sub></b>	0.154 <sub>±.000</sub>
Weather	Transf.	<b>0.153<sub>±.001</sub></b>	0.177 <sub>±.002</sub>
	Crossformer	<b>0.154<sub>±.003</sub></b>	0.164 <sub>±.003</sub>
	TimeMixer	<b>0.164<sub>±.002</sub></b>	0.178 <sub>±.001</sub>
	iTransformer	<b>0.154<sub>±.000</sub></b>	0.170 <sub>±.001</sub>
Traffic	Transf.	0.417 <sub>±.009</sub>	<b>0.392<sub>±.000</sub></b>
	Crossformer	0.540 <sub>±.014</sub>	<b>0.512<sub>±.007</sub></b>
	TimeMixer	0.464 <sub>±.001</sub>	<b>0.463<sub>±.001</sub></b>
	iTransformer	0.435 <sub>±.002</sub>	<b>0.409<sub>±.000</sub></b>
Solar	Transf.	<b>0.196<sub>±.000</sub></b>	0.205 <sub>±.001</sub>
	Crossformer	0.177 <sub>±.008</sub>	<b>0.166<sub>±.005</sub></b>
	TimeMixer	<b>0.366<sub>±.017</sub></b>	0.367 <sub>±.017</sub>
	iTransformer	<b>0.189<sub>±.001</sub></b>	0.197 <sub>±.002</sub>

uses learnable local parameters in the normalization module; Salinas et al. [2020]—while relying on an otherwise global model—uses a different one-hot-encoding vector associated with each processed time series, effectively introducing a vector of learnable parameters specific to that input sequence. Finally, an opposite trend seen in other approaches—often relying on simple (linear) models [Zeng et al., 2023]—design models in Eq. 2 by using different parameters for each time series

$$\hat{x}_{t:t+H}^i = \mathcal{F}(\mathbf{x}_{t-W:t}^i, \dots; \boldsymbol{\theta}^i) \quad \forall i = 1, \dots, N, \quad (5)$$

hence yielding to *local models*. Clearly, models in Eq. 2–5 correspond to fundamentally different approaches that can result in markedly different performance. Failing to recognize the impact of the associated design choices can be problematic for several reasons. First, the use of shared versus local parameters may have very different effects depending on whether the time series are homogeneous (e.g., data coming from identical sensors at different locations) or heterogeneous (e.g., measurements of different physical quantities). Moreover, when dealing with multiple multivariate time series, a multivariate global model is often more appropriate than a univariate one that processes channels independently. Second, as we will see, comparing the results of models belonging to different typologies without stating it explicitly can make it difficult to interpret performance differences. For example, comparing an architecture designed for an inductive setting with one evaluated in a transductive setting might disadvantage the first one, as the inductive models may be subject to additional constraints precisely to enable the processing of unseen time series. In Tab. 1, we assess the performance—in terms of mean square error (MSE)—of different architectures from the literature on a set of benchmarks (see Sec. 3.3). As in all our experiments, we focus on the task of long-range time series forecasting. We evaluate changes in performance for the reference Transformer and for two architectures that incorporate local parameters by removing these components, and, conversely, for the iTransformer by adding them. As one would expect, using local parameters drastically changes the observed results. Mixing results from the two columns without accounting for the impact of these design choices would clearly lead to misleading conclusions. Therefore, when aiming to identify the most effective sequence modeling operators, experiments should be designed to factor out the impact of model configuration.

## 4.2 Design dimension 2: Preprocessing and exogenous variables

Exogenous variables and preprocessing (e.g., scaling, detrending, and methods accounting for seasonality) are ingredients that can have a significant impact on final performance. In this section, we discuss how exogenous variables and preprocessing methods have been considered and included inconsistently across popular baselines and benchmarks. Similar to model configuration, these benchmarking practices further prevent a clear understanding of the reasons behind the observed performances. This issue is compounded by the growing trend of comparing newly proposed architectures directly against published results of existing methods, without reproducing those results in this exercise. It follows that differences in preprocessing routines become increasingly difficult to isolate and account for. To investigate the extent of this problem in recent benchmarks, we focus specifically on the use of exogenous variables. For instance, PatchTST, DLinear, and Crossformer do not use covariates by default, while iTransformer does. We then evaluate the impact of adding the same covariates (calendar features, in this case) to some of these baselines and report the outcome of this experiment in Tab. 2. Results show the impact of including covariates on the performance of models such as DLinear, PatchTST, and Crossformer, as well as removing them from iTransformer and the reference Transformer. Their effect is more pronounced on some benchmarks while less evident in others. These results pinpoint another source of uncertainty in interpreting recent benchmarking results; preprocessing steps should be standardized across baselines to ensure that all models have access to the same inputs.

Table 2: Comparison (MSE) of models with and without covariates for a forecasting horizon of 96. Best average results are in **bold**

	Model	w/ exog.	w/out exog.
Electr.	Transf.	<b>0.136<math>\pm</math>.000</b>	0.155 $\pm$ .001
	PatchTST	<b>0.128<math>\pm</math>.000</b>	0.134 $\pm$ .000
	Crossformer	<b>0.139<math>\pm</math>.002</b>	0.141 $\pm$ .001
	iTransformer	<b>0.154<math>\pm</math>.000</b>	0.167 $\pm$ .000
	DLinear	<b>0.193<math>\pm</math>.000</b>	0.195 $\pm$ .000
Weather	Transf.	<b>0.153<math>\pm</math>.001</b>	0.161 $\pm$ .000
	PatchTST	<b>0.174<math>\pm</math>.000</b>	0.180 $\pm$ .002
	Crossformer	0.154 $\pm$ .003	0.154 $\pm$ .003
	iTransformer	<b>0.170<math>\pm</math>.001</b>	0.176 $\pm$ .000
	DLinear	0.199 $\pm$ .005	<b>0.196<math>\pm</math>.001</b>
Traffic	Transf.	<b>0.417<math>\pm</math>.009</b>	0.479 $\pm$ .006
	PatchTST	<b>0.355<math>\pm</math>.000</b>	0.383 $\pm$ .001
	Crossformer	0.548 $\pm$ .024	<b>0.540<math>\pm</math>.014</b>
	iTransformer	<b>0.409<math>\pm</math>.000</b>	0.444 $\pm$ .001
	DLinear	<b>0.609<math>\pm</math>.000</b>	0.648 $\pm$ .000
Solar	Transf.	<b>0.196<math>\pm</math>.000</b>	0.206 $\pm$ .003
	PatchTST	<b>0.196<math>\pm</math>.001</b>	0.225 $\pm$ .003
	Crossformer	<b>0.176<math>\pm</math>.006</b>	0.177 $\pm$ .008
	iTransformer	<b>0.197<math>\pm</math>.002</b>	0.221 $\pm$ .003
	DLinear	<b>0.246<math>\pm</math>.001</b>	0.285 $\pm$ .001

## 4.3 Design dimension 3: Temporal processing

In this section, we assess whether streamlined models, properly configured as hybrid global-local models with exogenous inputs and local embeddings, can achieve performance comparable to that of recent state-of-the-art models. This design dimension, concerning sequence modeling operators, has been the main focus of recent research. However, this line of work has produced contrasting results, leading to considerable confusion about which components effectively contribute

Table 3: Forecasting results (MSE and MAE) for a horizon of 96 steps for models *not including* spatial processing. Best average results are in **bold**, second best are underlined.

MODEL	Electricity		Weather		Traffic		Solar	
	MSE	MAE	MSE	MAE	MSE	MAE	MSE	MAE
Linear Global	0.140	0.237	0.174	0.234	0.410	0.282	0.222	0.291
Linear Local	0.134	0.230	<b>0.144</b>	0.209	0.426	0.298	0.223	0.295
MLP	<u>0.129<sub>±.000</sub></u>	0.225 <sub>±.000</sub>	0.148 <sub>±.001</sub>	0.198 <sub>±.000</sub>	0.376 <sub>±.000</sub>	0.253 <sub>±.001</sub>	0.194 <sub>±.003</sub>	<u>0.239<sub>±.002</sub></u>
RNN	0.147 <sub>±.001</sub>	0.247 <sub>±.001</sub>	<u>0.149<sub>±.001</sub></u>	0.203 <sub>±.001</sub>	0.390 <sub>±.007</sub>	0.275 <sub>±.002</sub>	0.200 <sub>±.003</sub>	0.246 <sub>±.004</sub>
TCN	0.130 <sub>±.000</sub>	0.224 <sub>±.000</sub>	0.148 <sub>±.000</sub>	0.200 <sub>±.001</sub>	0.364 <sub>±.003</sub>	0.253 <sub>±.002</sub>	<u>0.193<sub>±.004</sub></u>	0.243 <sub>±.005</sub>
Transf.	<u>0.129<sub>±.001</sub></u>	<u>0.222<sub>±.001</sub></u>	0.149 <sub>±.001</sub>	0.203 <sub>±.002</sub>	<u>0.362<sub>±.003</sub></u>	<u>0.249<sub>±.002</sub></u>	0.203 <sub>±.006</sub>	0.245 <sub>±.002</sub>
Pyraf.	<u>0.129<sub>±.001</sub></u>	0.224 <sub>±.001</sub>	0.148 <sub>±.001</sub>	0.199 <sub>±.001</sub>	0.365 <sub>±.002</sub>	0.251 <sub>±.003</sub>	<b>0.189<sub>±.003</sub></b>	<b>0.236<sub>±.004</sub></b>
TimeMixer	0.129 <sub>±.001</sub>	0.224 <sub>±.000</sub>	<u>0.147<sub>±.001</sub></u>	0.197 <sub>±.000</sub>	0.373 <sub>±.002</sub>	0.271 <sub>±.003</sub>	0.199 <sub>±.001</sub>	0.245 <sub>±.000</sub>
PatchTST	<b>0.125<sub>±.000</sub></b>	<b>0.218<sub>±.000</sub></b>	0.148 <sub>±.001</sub>	<b>0.195<sub>±.001</sub></b>	<b>0.345<sub>±.000</sub></b>	<b>0.234<sub>±.000</sub></b>	0.197 <sub>±.001</sub>	0.244 <sub>±.004</sub>
DLinear	0.140 <sub>±.000</sub>	0.237 <sub>±.000</sub>	0.173 <sub>±.000</sub>	0.232 <sub>±.001</sub>	0.407 <sub>±.000</sub>	0.283 <sub>±.000</sub>	0.246 <sub>±.001</sub>	0.331 <sub>±.000</sub>

to performance [Toner and Darlow, 2024, Zeng et al., 2023, Tan et al., 2024]. We focus on methods that only process inputs along the temporal dimension, while approaches that include components accounting for spatial dependencies are discussed in Sec. 4.4. For this analysis, we use the different reference architectures introduced in Sec. 3.2, and compare them against three popular and well-established baselines, namely DLinear, PatchTST, and TimeMixer, by using standardized inputs (including covariates), and hyperparameter tuning. We remark that the goal is not to determine which architecture performs best, but rather to assess the extent to which different temporal processing components influence the observed results. As shown in Tab. 3, no single model consistently outperforms the others. Moreover, reference architectures that rely on standard and simple operators obtain competitive performance against the state of the art across all the considered scenarios. These results challenge the effectiveness of current benchmarking practices in identifying the components responsible for performance improvements and in measuring the contribution brought by the different sequence modeling operators. Additionally, results show that, in many scenarios, choosing a specific sequence modeling operator is not the critical design choice. Analogous observations are confirmed in Sec. 4.4.

Note that in all experiments, we process data from the Weather dataset as if it were a collection of univariate time series, to show the effect of handling it as is commonly done in the literature. Interestingly, one of the best-performing models on Weather is the local OLS Linear model. This is not too surprising, since Weather is actually a multivariate time series with heterogeneous channels, and among the models in Tab. 3, that linear model is the only one that explicitly models each time series as heterogeneous. Although results do not provide a clear ordering of methods, we did observe that patching, which, as mentioned earlier, corresponds to applying a nonlinear convolutional filter over time, works well across both reference architectures and state-of-the-art baselines, providing a good approach for enabling the processing of long input windows. Hierarchical attention-based approaches (such as Pyraformer) also showed to be a viable option. Finally, we report in Fig. 1 an assessment of the computational scalability of the different architectures, in terms of time needed to process each batch and GPU memory usage. The computational cost is visualized in relation to the forecasting accuracy. Results show that MLP, TCN, and PatchTST achieve a good trade-off between MSE performance, GPU memory usage, and training time.

#### 4.4 Design dimension 4: Spatial processing

We call *spatial* the dimension that spans multiple time series, which may correspond to different spatial locations when considering physical sensors. This section complements the discussion started in Sec. 4.3 by considering models that account for inter-series dependencies by relying on different operators. In particular, we compare the reference architectures, where dependencies are modeled with a standard spatial Transformer, against three state-of-the-art baselines: iTransformer, Crossformer, and ModernTCN. For the reference architectures, we use an MLP or pyramidal attention for temporal processing. Tab. 5 reports the results of the comparison, where we reduced the length of the input window associated with each time series to keep computational costs manageable. Analogously to Sec. 4.3, simulations show that the simple, streamlined architectures perform comparably

Table 4: Results (MSE) for iTransformer with or without space attention. Best average results are in **bold**.

Dataset	iTransformer	
	Space att.	Feedforward
Electricity	<b>0.148<sub>±.000</sub></b>	0.149 <sub>±.001</sub>
Weather	<b>0.171<sub>±.001</sub></b>	<b>0.171<sub>±.000</sub></b>
Traffic	0.393 <sub>±.001</sub>	<b>0.390<sub>±.001</sub></b>
Solar	0.208 <sub>±.003</sub>	<b>0.194<sub>±.001</sub></b>

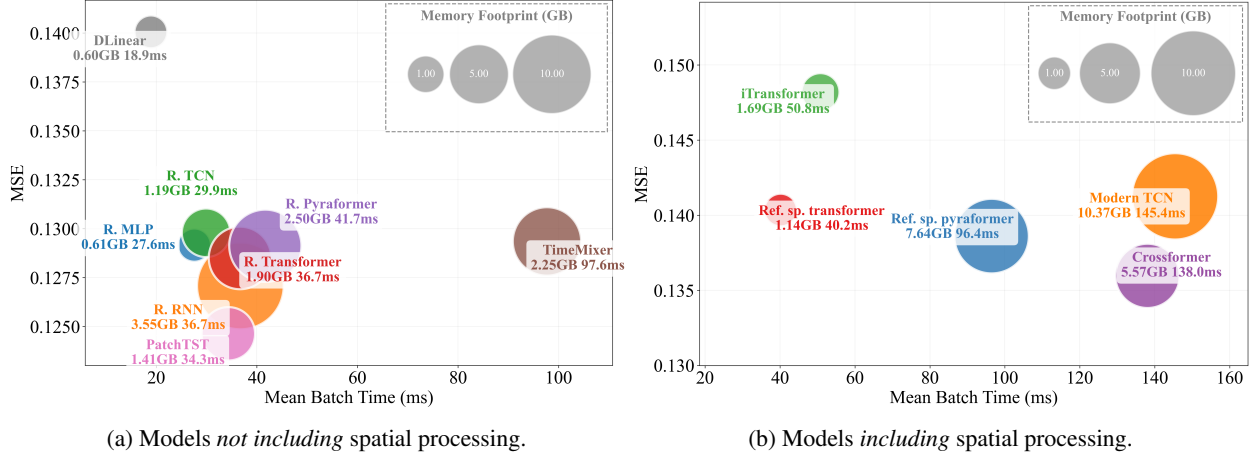


Figure 1: MSE versus mean batch time during training on the Electricity dataset for a forecasting horizon of 96. Circle size indicates memory consumption.

Table 5: Forecasting results (MSE and MAE) for a horizon of 96 steps for models *including* spatial processing. Best average results are in **bold**, second best are underlined.

Model	Electricity		Weather		Traffic		Solar	
	MSE	MAE	MSE	MAE	MSE	MAE	MSE	MAE
MLP + sp. attn.	$0.140 \pm .001$	$0.238 \pm .001$	$0.157 \pm .000$	$0.202 \pm .001$	$0.435 \pm .006$	$0.275 \pm .001$	$0.201 \pm .009$	$0.246 \pm .003$
Pyraf. + sp. attn.	$0.139 \pm .001$	$0.236 \pm .001$	$0.157 \pm .002$	$0.204 \pm .001$	$0.389 \pm .002$	$0.267 \pm .001$	$0.188 \pm .002$	$0.235 \pm .003$
iTransformer	$0.148 \pm .000$	$0.241 \pm .000$	$0.171 \pm .001$	$0.210 \pm .001$	$0.393 \pm .001$	<b><math>0.266 \pm .001</math></b>	$0.208 \pm .003$	$0.240 \pm .006$
Crosformer	<b><math>0.136 \pm .000</math></b>	<b><math>0.232 \pm .001</math></b>	<b><math>0.152 \pm .003</math></b>	$0.222 \pm .004$	$0.527 \pm .002$	$0.270 \pm .003$	<b><math>0.184 \pm .008</math></b>	$0.227 \pm .006$
ModernTCN	$0.141 \pm .000$	$0.237 \pm .001$	$0.154 \pm .001$	<b><math>0.200 \pm .001</math></b>	$0.445 \pm .001$	$0.287 \pm .001$	$0.190 \pm .001$	<b><math>0.222 \pm .002</math></b>

to the state of the art, highlighting once again the limitations of current benchmarking practices. The results in Tab. 3 and Tab. 5 combined with the observation that spatial dependencies might provide limited benefits in long-range forecasting, have led us to doubt the effectiveness of spatial attention operators in this context. For this reason, we design an additional architecture by replacing the spatial attention layer in iTransformer with a simple MLP, effectively removing all the components modeling spatial dependencies in the architecture. Surprisingly, the results in Tab. 4 show that in this context, entirely removing spatial attention led to better or similar performance in all the considered datasets. These observations further highlight the need for more thorough assessments of how each component contributes to the observed results. Finally, Fig. 1 reports performance in relation to computational cost, which in this case is particularly critical as processing data along the spatial dimension can have a significant impact on computational scalability.

## 5 Discussion

The results in Sec. 4.1–4.4 question whether we have been successful in measuring the advances of deep learning architectures for time series forecasting and shed light on several faults in current benchmarking practices. We showed that overlooked design choices can have a significant impact and that simple, well-designed architectures can match the state of the art on standard benchmarks (see Tab. 3 and Tab. 5). Our analysis calls for reaching a better understanding of the architecture’s design space, showing how misconceptions in model specification can trigger misleading conclusions (as shown, e.g., in Tab. 1). The additional ablation studies (e.g., in Tab. 2 and Tab. 4) corroborate these findings that are further substantiated by plenty of additional empirical results in the App. D of the paper. However, our objective is not to be dismissive of the progress of the field—which is tangible in many applications—but rather to ensure that we can move forward by focusing on answering foundational questions and fostering awareness of the existing flaws in our practices. A crucial step in this direction is to revise the benchmarking pipeline to account for all the main design dimensions and ensure that the empirical evaluation is effective by quantitatively assessing the improvement that the proposed designs bring to the state of the art. For instance, introducing benchmarks specifically

designed to isolate distinct dimensions, possibly by relying on synthetic datasets, can help measure the isolated effects of different design choices. Moreover, model cards [Mitchell et al., 2019] can be an effective tool, providing a simple and practical way to summarize a model’s main characteristics and to facilitate model comparison. Below, we propose an *auxiliary forecasting model card* that can be used in conjunction with existing model cards to capture relevant aspects of the design dimensions discussed in the paper, and we provide an example of its use in App. F. By providing a structured framework for documenting these aspects, the forecasting model card promotes transparency, reproducibility, and more informed comparisons across forecasting methods by helping users fully understand the characteristics of the model, reducing the time and effort required to extract such information from code or supplementary materials. We believe that by recalibrating our evaluation tools on reliably measuring actual progress, the shift toward answering more foundational methodological questions would happen as a natural consequence.

## FORECASTING MODEL CARD

### **Model setting**

- Size of the input window
- Whether the model is transductive or inductive, and can be used in a cold start scenario
- How to mask missing observations and/or if imputation is needed

### **D1. Model configuration**

- Whether the model is global, local, or hybrid
- *If the model is hybrid*, which parameters are shared across the time series and which are not

### **D2. Preprocessing and exogenous variables**

- The type of scaling or other transformation applied at training and inference time
- Temporal covariates, lagged variables, or other types of exogenous variables are employed

### **D3. Temporal processing**

- Modules and operators used to encode observations along the temporal axis
- Time and space complexity w.r.t. the length of the time series being processed

### **D4. Spatial processing**

*If spatial dependencies are accounted for:*

- Modules used to model spatial dynamics and whether a graph structure is employed
- Time and space complexity w.r.t. the number of the time series being processed

## 6 Conclusion

We investigated the effectiveness of current benchmarks in measuring progress in the field and the impact of design choices on forecasting performance. We showed, by analyzing points of failure in our evaluation procedures, that our current practices might produce misleading results. With this paper, we pinpointed several of the sources of this uncertainty and aimed to foster a discussion to ensure that the field can move forward and address its current limitations. Indeed, our analysis also shows that appropriate design choices do have an impact on performance and can explain seemingly contradictory and unexpected empirical results. We believe that the results and the analysis presented in this paper are an important step toward focusing on *what matters* in deep learning for time series forecasting.

**Limitations** In this work, we focused on a specific set of dimensions within the design space of forecasting models that have had a strong impact on the benchmarking results of recent studies. Clearly, this analysis can be extended to other aspects of the design space. For example, the discussion can be expanded to include probabilistic forecasting and the choice of metrics to quantify forecasting accuracy. Additionally, one could explore similar issues in short-term forecasting benchmarks and include a wider selection of settings and baselines. However, the purpose of this work is not to identify the best-performing architecture for different tasks, but rather to highlight how shortcomings in current evaluation practices can lead to misleading conclusions and unreliable performance assessment.

## References

S. Bai, J. Z. Kolter, and V. Koltun. An empirical evaluation of generic convolutional and recurrent networks for sequence modeling. *arXiv preprint arXiv:1803.01271*, 2018.

M. Bechler-Speicher, B. Finkelshtein, F. Frasca, L. Müller, J. Tönshoff, A. Siraudin, V. Zaverkin, M. M. Bronstein, M. Niepert, B. Perozzi, M. Galkin, and C. Morris. Position: Graph learning will lose relevance due to poor benchmarks. In *Forty-second International Conference on Machine Learning Position Paper Track*, 2025. URL <https://openreview.net/forum?id=nDFp121hoH>.

M. Beck, K. Pöppel, M. Spanring, A. Auer, O. Prudnikova, M. Kopp, G. Klambauer, J. Brandstetter, and S. Hochreiter. xlstm: Extended long short-term memory. *Advances in Neural Information Processing Systems*, 37:107547–107603, 2024.

K. Benidis, S. S. Rangapuram, V. Flunkert, Y. Wang, D. Maddix, C. Turkmen, J. Gasthaus, M. Bohlke-Schneider, D. Salinas, L. Stella, F.-X. Aubet, L. Callot, and T. Januschowski. Deep learning for time series forecasting: Tutorial and literature survey. *ACM Comput. Surv.*, 55(6), dec 2022. ISSN 0360-0300. doi: 10.1145/3533382. URL <https://doi.org/10.1145/3533382>.

L. Brigato, R. Morand, K. Strømmen, M. Panagiotou, M. Schmidt, and S. Mougiakakou. Position: There are no champions in long-term time series forecasting, 2025. URL <https://arxiv.org/abs/2502.14045>.

J. Chung, C. Gulcehre, K. Cho, and Y. Bengio. Empirical evaluation of gated recurrent neural networks on sequence modeling. *arXiv preprint arXiv:1412.3555*, 2014.

A. Cini and I. Marisca. Torch Spatiotemporal, 3 2022. URL <https://github.com/TorchSpatiotemporal/tsl>.

A. Cini, I. Marisca, D. Zambon, and C. Alippi. Taming local effects in graph-based spatiotemporal forecasting. *Advances in Neural Information Processing Systems*, 36:55375–55393, 2023.

L. Donghao and W. Xue. ModernTCN: A modern pure convolution structure for general time series analysis. In *The Twelfth International Conference on Learning Representations*, 2024. URL <https://openreview.net/forum?id=vpJMJerXHU>.

V. P. Dwivedi, C. K. Joshi, A. T. Luu, T. Laurent, Y. Bengio, and X. Bresson. Benchmarking graph neural networks. *Journal of Machine Learning Research*, 24(43):1–48, 2023.

F. Errica, M. Podda, D. Bacciu, and A. Micheli. A fair comparison of graph neural networks for graph classification. In *Proceedings of the 8th International Conference on Learning Representations (ICLR)*, 2020.

W. Falcon and The PyTorch Lightning team. PyTorch Lightning, 3 2019. URL <https://github.com/PyTorchLightning/pytorch-lightning>.

M. Fey and J. E. Lenssen. Fast graph representation learning with PyTorch Geometric. In *ICLR Workshop on Representation Learning on Graphs and Manifolds*, 2019.

M. Fey, J. Sunil, A. Nitta, R. Puri, M. Shah, B. Stojanović, R. Bendias, B. Alexandria, V. Kocijan, Z. Zhang, X. He, J. E. Lenssen, and J. Leskovec. PyG 2.0: Scalable learning on real world graphs. In *Temporal Graph Learning Workshop @ KDD*, 2025.

J. Grigsby, Z. Wang, N. Nguyen, and Y. Qi. Long-range transformers for dynamic spatiotemporal forecasting. *arXiv preprint arXiv:2109.12218*, 2021.

A. Gu and T. Dao. Mamba: Linear-time sequence modeling with selective state spaces. In *First Conference on Language Modeling*, 2024.

A. Gu, K. Goel, and C. Re. Efficiently modeling long sequences with structured state spaces. In *International Conference on Learning Representations*, 2022. URL <https://openreview.net/forum?id=uYLFoZ1v1AC>.

C. R. Harris, K. J. Millman, S. J. Van Der Walt, R. Gommers, P. Virtanen, D. Cournapeau, E. Wieser, J. Taylor, S. Berg, N. J. Smith, et al. Array programming with numpy. *Nature*, 585(7825):357–362, 2020.

M. Herrmann, F. J. D. Lange, K. Eggensperger, G. Casalicchio, M. Wever, M. Feurer, D. Rügamer, E. Hüllermeier, A.-L. Boulesteix, and B. Bischl. Position: Why we must rethink empirical research in machine learning. In R. Salakhutdinov, Z. Kolter, K. Heller, A. Weller, N. Oliver, J. Scarlett, and F. Berkenkamp, editors, *Proceedings of the 41st International Conference on Machine Learning*, volume 235 of *Proceedings of Machine Learning Research*, pages 18228–18247. PMLR, 21–27 Jul 2024. URL <https://proceedings.mlr.press/v235/herrmann24b.html>.

H. Hewamalage, C. Bergmeir, and K. Bandara. Recurrent neural networks for time series forecasting: Current status and future directions. *International Journal of Forecasting*, 37(1):388–427, 2021.

T. Januschowski, J. Gasthaus, Y. Wang, D. Salinas, V. Flunkert, M. Bohlke-Schneider, and L. Callot. Criteria for classifying forecasting methods. *International Journal of Forecasting*, 36(1):167–177, 2020.

T. Kim, J. Kim, Y. Tae, C. Park, J.-H. Choi, and J. Choo. Reversible instance normalization for accurate time-series forecasting against distribution shift. In *International Conference on Learning Representations*, 2022. URL <https://openreview.net/forum?id=cGDAkQo1C0p>.

M. Kunz, S. Birr, M. Raslan, L. Ma, and T. Januschowski. Deep learning based forecasting: a case study from the online fashion industry. In *Forecasting with artificial intelligence: theory and applications*, pages 279–311. Springer, 2023.

G. Lai, W.-C. Chang, Y. Yang, and H. Liu. Modeling long-and short-term temporal patterns with deep neural networks. In *The 41st international ACM SIGIR conference on research & development in information retrieval*, pages 95–104, 2018.

H. Liu, Z. Dong, R. Jiang, J. Deng, J. Deng, Q. Chen, and X. Song. Spatio-temporal adaptive embedding makes vanilla transformer sota for traffic forecasting. In *Proceedings of the 32nd ACM international conference on information and knowledge management*, pages 4125–4129, 2023a.

S. Liu, H. Yu, C. Liao, J. Li, W. Lin, A. X. Liu, and S. Dustdar. Pyraformer: Low-complexity pyramidal attention for long-range time series modeling and forecasting. In *International Conference on Learning Representations*, 2022a. URL <https://openreview.net/forum?id=0EXmFzUn5I>.

Y. Liu, H. Wu, J. Wang, and M. Long. Non-stationary transformers: Exploring the stationarity in time series forecasting. *Advances in neural information processing systems*, 35:9881–9893, 2022b.

Y. Liu, T. Hu, H. Zhang, H. Wu, S. Wang, L. Ma, and M. Long. itransformer: Inverted transformers are effective for time series forecasting. *arXiv preprint arXiv:2310.06625*, 2023b.

J. Ma, Z. Shou, A. Zareian, H. Mansour, A. Vetro, and S.-F. Chang. Cdsa: cross-dimensional self-attention for multivariate, geo-tagged time series imputation. *arXiv preprint arXiv:1905.09904*, 2019.

I. Marasca, A. Cini, and C. Alippi. Learning to Reconstruct Missing Data from Spatiotemporal Graphs with Sparse Observations. In *Advances in Neural Information Processing Systems*, 2022.

M. Mitchell, S. Wu, A. Zaldivar, P. Barnes, L. Vasserman, B. Hutchinson, E. Spitzer, I. D. Raji, and T. Gebru. Model cards for model reporting. In *Proceedings of the conference on fairness, accountability, and transparency*, pages 220–229, 2019.

P. Montero-Manso and R. J. Hyndman. Principles and algorithms for forecasting groups of time series: Locality and globality. *International Journal of Forecasting*, 37(4):1632–1653, 2021.

Y. Nie, N. H. Nguyen, P. Sinthong, and J. Kalagnanam. A time series is worth 64 words: Long-term forecasting with transformers. In *International Conference on Learning Representations*, 2023.

A. Orvieto, S. L. Smith, A. Gu, A. Fernando, C. Gulcehre, R. Pascanu, and S. De. Resurrecting recurrent neural networks for long sequences. In *International Conference on Machine Learning*, pages 26670–26698. PMLR, 2023.

A. Paszke, S. Gross, F. Massa, A. Lerer, J. Bradbury, G. Chanan, N. Gimelshein, L. Antiga, A. Desmaison, A. Kopf, E. Yang, Z. DeVito, M. Raison, A. Tejani, S. Chilamkurthy, B. Steiner, L. Fang, J. Bai, and S. Chintala. Pytorch: An imperative style, high-performance deep learning library. In H. Wallach, H. Larochelle, A. Beygelzimer, F. d'Alché-Buc, E. Fox, and R. Garnett, editors, *Advances in Neural Information Processing Systems 32*, pages 8024–8035. Curran Associates, Inc., 2019.

F. Pedregosa, G. Varoquaux, A. Gramfort, V. Michel, B. Thirion, O. Grisel, M. Blondel, P. Prettenhofer, R. Weiss, V. Dubourg, et al. Scikit-learn: Machine learning in python. *Journal of Machine Learning Research*, 12:2825–2830, 2011.

X. Qiu, J. Hu, L. Zhou, X. Wu, J. Du, B. Zhang, C. Guo, A. Zhou, C. S. Jensen, Z. Sheng, et al. Tfb: Towards comprehensive and fair benchmarking of time series forecasting methods. *CoRR*, 2024.

A. Raichuk, P. Stańczyk, M. Orsini, S. Girgin, R. Marinier, L. Hussenot, M. Geist, O. Pietquin, M. Michalski, and S. Gelly. What matters for on-policy deep actor-critic methods? a large-scale study. In *International Conference on Learning Representations*, 2021. URL <https://api.semanticscholar.org/CorpusID:233340556>.

D. Salinas, V. Flunkert, J. Gasthaus, and T. Januschowski. Deepar: Probabilistic forecasting with autoregressive recurrent networks. *International Journal of Forecasting*, 36(3):1181–1191, 2020.

R. Sen, H.-F. Yu, and I. S. Dhillon. Think globally, act locally: A deep neural network approach to high-dimensional time series forecasting. *Advances in neural information processing systems*, 32, 2019.

Z. Shao, Z. Zhang, F. Wang, W. Wei, and Y. Xu. Spatial-temporal identity: A simple yet effective baseline for multivariate time series forecasting. In *Proceedings of the 31st ACM international conference on information & knowledge management*, pages 4454–4458, 2022.

Z. Shao, F. Wang, Y. Xu, W. Wei, C. Yu, Z. Zhang, D. Yao, T. Sun, G. Jin, X. Cao, et al. Exploring progress in multivariate time series forecasting: Comprehensive benchmarking and heterogeneity analysis. *IEEE Transactions on Knowledge and Data Engineering*, 2024.

S. Smyl. A hybrid method of exponential smoothing and recurrent neural networks for time series forecasting. *International journal of forecasting*, 36(1):75–85, 2020.

M. Tan, M. A. Merrill, V. Gupta, T. Althoff, and T. Hartvigsen. Are language models actually useful for time series forecasting? In *The Thirty-eighth Annual Conference on Neural Information Processing Systems*, 2024. URL <https://openreview.net/forum?id=DV15UbHCY1>.

W. Toner and L. N. Darlow. An analysis of linear time series forecasting models. In *International Conference on Machine Learning*, pages 48404–48427. PMLR, 2024.

G. Van Rossum and F. L. Drake. *Python 3 Reference Manual*. CreateSpace, Scotts Valley, CA, 2009. ISBN 1441412697.

A. Vaswani, N. Shazeer, N. Parmar, J. Uszkoreit, L. Jones, A. N. Gomez, Ł. Kaiser, and I. Polosukhin. Attention is all you need. *Advances in neural information processing systems*, 30, 2017.

S. Wang, H. Wu, X. Shi, T. Hu, H. Luo, L. Ma, J. Y. Zhang, and J. ZHOU. Timemixer: Decomposable multiscale mixing for time series forecasting. In *International Conference on Learning Representations (ICLR)*, 2024a.

Y. Wang, A. Smola, D. Maddix, J. Gasthaus, D. Foster, and T. Januschowski. Deep factors for forecasting. In *International conference on machine learning*, pages 6607–6617. PMLR, 2019.

Y. Wang, H. Wu, J. Dong, Y. Liu, M. Long, and J. Wang. Deep time series models: A comprehensive survey and benchmark. 2024b.

H. Wu, J. Xu, J. Wang, and M. Long. Autoformer: Decomposition transformers with Auto-Correlation for long-term series forecasting. In *Advances in Neural Information Processing Systems*, 2021.

H. Wu, T. Hu, Y. Liu, H. Zhou, J. Wang, and M. Long. Timesnet: Temporal 2d-variation modeling for general time series analysis. In *International Conference on Learning Representations*, 2023.

O. Yadan. Hydra - a framework for elegantly configuring complex applications. Github, 2019. URL <https://github.com/facebookresearch/hydra>.

A. Zeng, M. Chen, L. Zhang, and Q. Xu. Are transformers effective for time series forecasting? In *Proceedings of the AAAI conference on artificial intelligence*, volume 37, pages 11121–11128, 2023.

G. Zhang, B. E. Patuwo, and M. Y. Hu. Forecasting with artificial neural networks:: The state of the art. *International journal of forecasting*, 14(1):35–62, 1998.

Y. Zhang and J. Yan. Crossformer: Transformer utilizing cross-dimension dependency for multivariate time series forecasting. In *The Eleventh International Conference on Learning Representations*, 2023. URL <https://openreview.net/forum?id=vSVLM2j9eie>.

H. Zhou, S. Zhang, J. Peng, S. Zhang, J. Li, H. Xiong, and W. Zhang. Informer: Beyond efficient transformer for long sequence time-series forecasting. In *Proceedings of the AAAI conference on artificial intelligence*, volume 35, pages 11106–11115, 2021.

T. Zhou, Z. Ma, Q. Wen, X. Wang, L. Sun, and R. Jin. FEDformer: Frequency enhanced decomposed transformer for long-term series forecasting. In *Proc. 39th International Conference on Machine Learning (ICML 2022)*, 2022.

## Appendix

### A Baselines

Below, we provide a brief description of each baseline as employed in our experiments on the considered benchmarks. Furthermore, we summarize them in Tab. 6 using three fields corresponding to the design dimensions introduced in Sec. 4, excluding the *preprocessing and exogenous variables* dimension due to the considerable differences among the methods.

- Dlinear [Zeng et al., 2023] decomposes the input into seasonal and trend components using a moving average and processes them with linear layers. The hyperparameters determine its local-global nature. In the table, we report it as global because, in our experiments, it was used in this configuration. We follow the same convention for PatchTST and TimeMixer.

Table 6: Description for the baseline models

Model	Model configuration	Temporal processing	Spatial processing
Dlinear	Global	Linear layers	Not modeled
PatchTST	Global	Temporal convolution followed by temporal attention over the patches	Not modeled
TimeMixer	Hybrid	Feedforward networks applied to the trend and seasonal components, downsampled at different scales	Not modeled
Crossformer	Hybrid	Temporal convolution followed by attention applied over the patches, with a hierarchical structure constructed with linear layers	Spatial attention applied among patches of different time series
iTransformer	Global	Feedforward layers	Spatial attention applied among different time series
ModernTCN	Hybrid	Depth-wise convolutions	Convolution applied across time series
Linear global/local	Global/local	Linear autoregression	Not modeled

- PatchTST [Nie et al., 2023] has strongly influenced subsequent works by employing a global Transformer, in contrast to earlier local multivariate approaches that treated the group of input time series as a single multivariate series. PatchTST segments the time series and generates corresponding embeddings using an operation analogous to temporal convolution. Then, it applies attention over these segments, referred to as *patches*. It does not model spatial relations.
- TimeMixer [Wang et al., 2024a] is a fully MLP-based architecture that downsamples the input at different scales, decomposes it into trend and seasonal components, and employs feedforward layers to model temporal dependencies.
- Crossformer [Zhang and Yan, 2023] employs an input encoding with segmentation analogous to that used in PatchTST. The model is a hybrid global-local model, as it includes learnable position embeddings for each time series in the set. In addition to temporal attention, it captures spatial dependencies through attention over the spatial dimension using a routing mechanism. Furthermore, it adopts a hierarchical encoder-decoder structure.
- iTransformer [Liu et al., 2023b] is a global model that uses a feedforward approach to encode temporal dynamics and spatial attention to model spatial dependencies. This method has been described as applying attention to the *inverted dimension*, i.e., the spatial dimension. The model is global.
- ModernTCN [Donghao and Xue, 2024] uses depth-wise convolutions to encode temporal information, with an encoding similar to that performed in PatchTST, and then applies point-wise convolutions to process the feature and spatial dimensions separately.
- Linear [Toner and Darlow, 2024] is linear autoregressive models trained with  $L2$  regularization and OLS. The *local* variant employs different weights for each series, while the *global* variant employs the same weights for all the series in the set.

## B Reference architectures structure

The reference architectures, as schematized in Fig. 2, consist of a preprocessing module, followed by the processing of the temporal and spatial dynamics, and finally a postprocessing module. Their modular structure facilitates understanding of the architecture and promotes fair comparisons, as each module can be modified independently. In our experiments, we kept most modules fixed, modifying only the temporal and spatial modules for the experiments reported in Sec. 4.3 and 4.4, respectively, and occasionally the feature encoding module. Here, we provide a more detailed description, complementing Sec. 3.2.

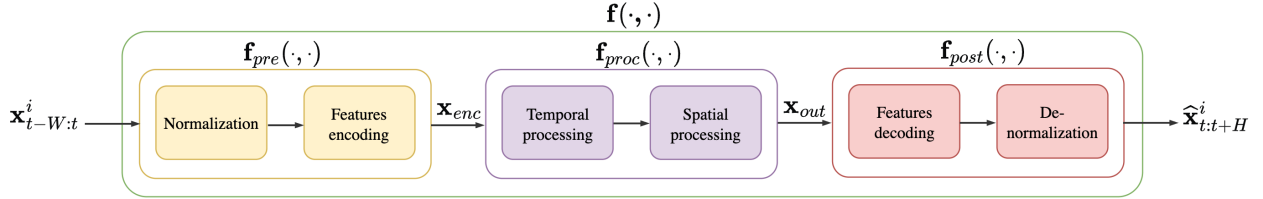


Figure 2: Block diagram of the reference architectures

**Preprocessing module** The preprocessing module begins with RevInv [Kim et al., 2022] normalization. Then, the feature encoding module processes the input and covariates through non-linear layers and returns their sum. Alternatively, it can perform temporal convolution to generate an encoding similar to that in [Nie et al., 2023]. Finally, local embeddings are concatenated with the resulting encoding.

**Processing module** The processing module consists of temporal processing followed by spatial processing. In a more general architecture, these components could be interleaved. For simplicity, however, they are treated separately in our implementation.

**Postprocessing module** The postprocessing module consists of a linear decoder that maps the hidden representations to predictions for the horizon. Finally, the predictions are de-normalized using the RevInv module.

## C Hyperparameter tuning

For each experiment, we set a fixed batch size for each dataset. The hidden size is tuned between 32 and 256 for all datasets, with the addition of 16 for the Weather dataset. For the Tables and Figures in Sec. 4.3, Sec. 4.4, Tab. 11 –Tab. 17 and Fig. 3, Fig. 4 we used the hyperparameters of the best-performing configuration identified during tuning for each considered window size for a 96-step forecasting horizon. Instead, hyperparameters in Tab. 1, Tab. 2, Tab. 8 and Tab. 10 are fixed and identical for both sides of the comparison. In Tab. 3, Tab. 12, and Fig. 3, the window size was set to 336 for all datasets except Solar. Throughout the paper, unless otherwise specified, the window size and the forecasting horizon are set to 96.

## D Empirical setup and additional experiments

In this section, we provide further details on the experiments conducted in Sec. 4.1 –Sec. 4.4. Moreover, we present additional experiments and extend the tables from the paper by including the mean absolute error (MAE) metric, additional forecasting horizons and window sizes. Additional information on the datasets is provided in Tab. 7.

Table 7: Information on the datasets.

Dataset	Time series	Steps	Frequency	Domain
Weather	21	52695	10min	Weather
Solar-Energy	137	52559	10min	Energy
ECL	321	26303	Hourly	Electricity
Traffic	862	17543	Hourly	Transportation

### D.1 Empirical setup and additional experiments for D1: Model configuration

To obtain the global version of models that include local parameters in the experiments of Sec. 4.1, we remove such local components. For example, the global TimeMixer model is obtained by removing the learnable parameters from the normalization module, while the global versions of Crossformer and the reference Transformer are obtained by removing their local embeddings. Conversely, to create a hybrid version of an otherwise global model, we add per-series local embeddings, which are used as an additional input, as done for iTransformer. This approach is straightforward and can be applied to different architectures, as also shown by recent works [Cini et al., 2023, Shao et al., 2022].

The results in Tab. 8 extend Tab. 1 for both MSE and MAE. We added in Tab. 9, a comparison of all the possible configurations—local, global, and hybrid—for linear models. The simple hybrid variants are obtained by concatenating learnable local parameters to the input for DLinear, and by concatenating a one-hot encoding representing the time series for Linear. The results are consistent with the findings discussed in Sec. 4.1.

Table 8: Comparison (MSE and MAE) of models with and without local parameters. Best average results are in **bold**.

D	Model	hybrid		global	
		MSE	MAE	MSE	MAE
Electr.	Transf.	<b>0.136<math>\pm</math>.000</b>	<b>0.231<math>\pm</math>.000</b>	0.151 $\pm$ .000	0.242 $\pm$ .000
	Crossformer	<b>0.141<math>\pm</math>.001</b>	<b>0.235<math>\pm</math>.001</b>	0.146 $\pm$ .003	0.240 $\pm$ .003
	TimeMixer	<b>0.151<math>\pm</math>.000</b>	<b>0.248<math>\pm</math>.001</b>	0.180 $\pm$ .001	0.268 $\pm$ .001
	iTransformer	<b>0.139<math>\pm</math>.000</b>	<b>0.236<math>\pm</math>.001</b>	0.154 $\pm$ .000	0.245 $\pm$ .000
Weather	Transf.	<b>0.153<math>\pm</math>.001</b>	<b>0.198<math>\pm</math>.000</b>	0.177 $\pm$ .002	0.215 $\pm$ .001
	Crossformer	<b>0.154<math>\pm</math>.003</b>	0.225 $\pm$ .004	0.164 $\pm$ .003	<b>0.224<math>\pm</math>.007</b>
	TimeMixer	<b>0.164<math>\pm</math>.002</b>	<b>0.208<math>\pm</math>.001</b>	0.178 $\pm$ .001	0.216 $\pm$ .001
	iTransformer	<b>0.154<math>\pm</math>.000</b>	<b>0.199<math>\pm</math>.001</b>	0.170 $\pm$ .001	0.211 $\pm$ .001
Traffic	Transf.	0.417 $\pm$ .009	0.278 $\pm$ .005	<b>0.392<math>\pm</math>.000</b>	<b>0.260<math>\pm</math>.001</b>
	Crossformer	0.540 $\pm$ .014	0.279 $\pm$ .007	<b>0.512<math>\pm</math>.007</b>	<b>0.259<math>\pm</math>.004</b>
	TimeMixer	0.464 $\pm$ .001	0.328 $\pm$ .003	<b>0.463<math>\pm</math>.001</b>	<b>0.327<math>\pm</math>.003</b>
	iTransformer	0.435 $\pm$ .002	<b>0.275<math>\pm</math>.000</b>	<b>0.409<math>\pm</math>.000</b>	0.277 $\pm$ .001
Solar	Transf.	<b>0.196<math>\pm</math>.000</b>	<b>0.243<math>\pm</math>.001</b>	0.205 $\pm$ .001	0.247 $\pm$ .002
	Crossformer	0.177 $\pm$ .008	0.215 $\pm$ .004	<b>0.166<math>\pm</math>.005</b>	<b>0.204<math>\pm</math>.006</b>
	TimeMixer	<b>0.366<math>\pm</math>.017</b>	<b>0.396<math>\pm</math>.013</b>	0.367 $\pm$ .017	0.396 $\pm$ .013
	iTransformer	<b>0.189<math>\pm</math>.001</b>	<b>0.240<math>\pm</math>.004</b>	0.197 $\pm$ .002	0.243 $\pm$ .001

Table 9: Comparison (MSE and MAE) of Linear models in their local, global, and hybrid variants. A dash (–) marks experiments beyond our computational budget. Best mean results are in **bold**.

Dataset	Model	Hybrid		Global		Local	
		MSE	MAE	MSE	MAE	MSE	MAE
Electr.	DLinear	0.195 $\pm$ .000	0.277 $\pm$ .000	0.195 $\pm$ .000	0.277 $\pm$ .000	<b>0.184<math>\pm</math>.000</b>	<b>0.270<math>\pm</math>.000</b>
	OLS	0.194 $\pm$ .000	0.277 $\pm$ .000	0.195 $\pm$ .000	0.277 $\pm$ .000	<b>0.184<math>\pm</math>.000</b>	<b>0.270<math>\pm</math>.000</b>
Weather	DLinear	0.198 $\pm$ .001	0.254 $\pm$ .002	0.196 $\pm$ .001	0.248 $\pm$ .002	<b>0.161<math>\pm</math>.001</b>	<b>0.233<math>\pm</math>.001</b>
	OLS	0.196 $\pm$ .000	0.254 $\pm$ .000	0.195 $\pm$ .000	0.253 $\pm$ .000	<b>0.161<math>\pm</math>.000</b>	<b>0.233<math>\pm</math>.000</b>
Traffic	DLinear	0.648 $\pm$ .000	<b>0.395<math>\pm</math>.000</b>	0.648 $\pm$ .000	<b>0.395<math>\pm</math>.000</b>	<b>0.647<math>\pm</math>.000</b>	0.403 $\pm$ .000
	OLS	-	-	0.649 $\pm$ .000	<b>0.396<math>\pm</math>.000</b>	<b>0.647<math>\pm</math>.000</b>	0.403 $\pm$ .000
Solar	DLinear	0.286 $\pm$ .000	0.375 $\pm$ .001	<b>0.285<math>\pm</math>.001</b>	<b>0.372<math>\pm</math>.001</b>	0.286 $\pm$ .000	0.376 $\pm$ .001
	OLS	<b>0.285<math>\pm</math>.000</b>	<b>0.372<math>\pm</math>.000</b>	<b>0.285<math>\pm</math>.000</b>	<b>0.372<math>\pm</math>.000</b>	0.286 $\pm$ .000	0.374 $\pm$ .000

## D.2 Empirical setup and additional experiments for D2: Preprocessing and exogenous variables

For the experiment in Sec. 4.2, covariates were removed from the models that originally used them in their implementations, such as the reference Transformer and iTransformer, and added to the models that did not include them, such as PatchTST, DLinear, and Crossformer. The results in Tab. 10 extend Tab. 2 for both MSE and MAE.

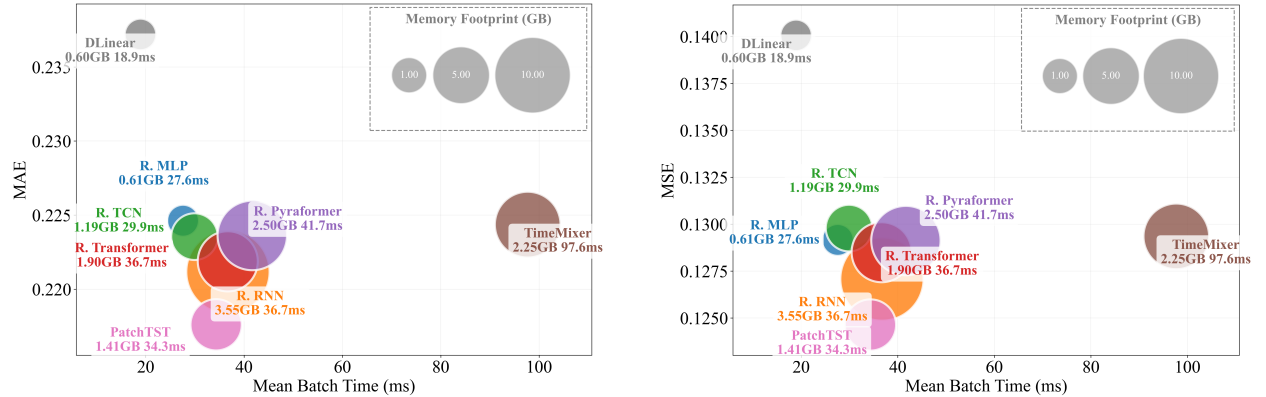
## D.3 Empirical setup and additional experiments for D3: Temporal processing

Results in Sec. 4.3 were obtained through extensive hyperparameter tuning for each model, configured with exogenous inputs as hybrid global-local embeddings. The results in Tab. 11 extend Tab. 3 to a broader set of horizons (96, 192, 336,

Table 10: Comparison (MSE and MAE) of models with and without covariates. Best average results are in **bold**.

D	Model	w/ exog.		w/o exog.	
		MSE	MAE	MSE	MAE
Electr.	Transf.	<b>0.136<sub>.000</sub></b>	<b>0.231<sub>.000</sub></b>	0.155 <sub>.001</sub>	0.247 <sub>.000</sub>
	PatchTST	<b>0.128<sub>.000</sub></b>	<b>0.222<sub>.000</sub></b>	0.134 <sub>.000</sub>	0.228 <sub>.001</sub>
	Crossformer	<b>0.139<sub>.002</sub></b>	<b>0.234<sub>.003</sub></b>	0.141 <sub>.001</sub>	0.235 <sub>.001</sub>
	iTransformer	<b>0.154<sub>.000</sub></b>	<b>0.245<sub>.000</sub></b>	0.167 <sub>.000</sub>	0.254 <sub>.000</sub>
	DLinear	<b>0.193<sub>.000</sub></b>	0.277 <sub>.000</sub>	0.195 <sub>.000</sub>	0.277 <sub>.000</sub>
Weather	Transf.	<b>0.153<sub>.001</sub></b>	<b>0.198<sub>.000</sub></b>	0.161 <sub>.000</sub>	0.208 <sub>.001</sub>
	PatchTST	<b>0.174<sub>.000</sub></b>	<b>0.213<sub>.001</sub></b>	0.180 <sub>.002</sub>	0.221 <sub>.002</sub>
	Crossformer	0.154 <sub>.003</sub>	0.225 <sub>.002</sub>	0.154 <sub>.003</sub>	0.225 <sub>.004</sub>
	iTransformer	<b>0.170<sub>.001</sub></b>	<b>0.211<sub>.001</sub></b>	0.176 <sub>.000</sub>	0.217 <sub>.001</sub>
	DLinear	0.199 <sub>.005</sub>	0.258 <sub>.008</sub>	<b>0.196<sub>.001</sub></b>	<b>0.248<sub>.002</sub></b>
Traffic	Transf.	<b>0.417<sub>.009</sub></b>	<b>0.278<sub>.005</sub></b>	0.479 <sub>.006</sub>	0.289 <sub>.001</sub>
	PatchTST	<b>0.355<sub>.000</sub></b>	<b>0.244<sub>.000</sub></b>	0.383 <sub>.001</sub>	0.261 <sub>.001</sub>
	Crossformer	0.548 <sub>.024</sub>	<b>0.278<sub>.011</sub></b>	<b>0.540<sub>.014</sub></b>	0.279 <sub>.007</sub>
	iTransformer	<b>0.409<sub>.000</sub></b>	<b>0.277<sub>.001</sub></b>	0.444 <sub>.001</sub>	0.290 <sub>.001</sub>
	DLinear	<b>0.609<sub>.000</sub></b>	<b>0.391<sub>.000</sub></b>	0.648 <sub>.000</sub>	0.395 <sub>.000</sub>
Solar	Transf.	<b>0.196<sub>.000</sub></b>	<b>0.243<sub>.001</sub></b>	0.206 <sub>.003</sub>	0.249 <sub>.004</sub>
	PatchTST	<b>0.196<sub>.001</sub></b>	<b>0.246<sub>.004</sub></b>	0.225 <sub>.003</sub>	0.268 <sub>.003</sub>
	Crossformer	<b>0.176<sub>.006</sub></b>	0.231 <sub>.010</sub>	0.177 <sub>.008</sub>	<b>0.215<sub>.004</sub></b>
	iTransformer	<b>0.197<sub>.002</sub></b>	<b>0.243<sub>.001</sub></b>	0.221 <sub>.003</sub>	0.256 <sub>.002</sub>
	DLinear	<b>0.246<sub>.001</sub></b>	<b>0.331<sub>.000</sub></b>	0.285 <sub>.001</sub>	0.372 <sub>.001</sub>

720). We observe that increasing the forecasting horizon does not change the conclusions drawn in the corresponding sections, and results still show that, even for larger forecasting horizons, standard, streamlined architectures achieve performance comparable to current state-of-the-art models. Tab. 12 shows the computational efficiency of the models for increasing horizons on the Electricity dataset. We employed the PyTorch Profiler [Paszke et al., 2019] to monitor GPU performance during training, specifically collecting the total CUDA execution time. Additionally, GPU memory usage was obtained using the PyG [Fey et al., 2025] function `get_gpu_memory_from_nvidia_smi`. To ensure a consistent evaluation, all measurements related to model performance (Tab. 12 and 18) were conducted on the same machine running Oracle Linux Server 8.8, equipped with an Intel Xeon E5-2650 v3 CPU @ 2.30 GHz 20 (2 x 10) cores, 128 GB of system RAM, and an NVIDIA A100-PCIe GPU with 40 GB of HBM2 memory. Finally, we summarize these results in Fig. 3, which illustrates the trade-off between model performance and computational efficiency in terms of training batch time and GPU memory usage, on the Electricity dataset for a forecasting horizon of 96.

Figure 3: MAE and MSE performance versus mean batch time during training for models *not including* spatial processing, for a batch size of 512. Circle size indicates memory consumption.

#### D.4 Empirical setup and additional experiments for D4: Spatial processing

Analogously to Sec. 4.3, results in Sec. 4.4 were obtained through extensive hyperparameter tuning for each model, configured with exogenous inputs as hybrid global-local embeddings. The results in Tab. 13 extend Tab. 5 for both MSE and MAE, comparing the performance of the reference architectures against baselines that include spatial processing. The reference architectures incorporate either a MLP or a pyramidal attention module for temporal processing, followed by a spatial attention module. The temporal modules were chosen for their advantageous trade-off between performance and computational efficiency (see Fig. 3 and Tab. 12). The ablation study in Tab. 5 compares iTransformer against its variant that replaces space attention with a simple feedforward layer. Tab. 14 – Tab. 17 expand the iTransformer ablation study to additional window sizes (96, 336, 720) and forecasting horizons (96, 336, 720) for both MSE and MAE. These additional experiments further reinforce our analysis in Sec. 4.4, showing a general performance improvement when removing one of the core components introduced by state-of-the-art architectures. Analogously to Tab. 12 and Fig. 3, Tab. 18 and Fig. 4 show the trade-off between model performance and computational efficiency on the Electricity dataset for a forecasting horizon of 96. Since spatial processing often increases computational cost and reduces memory efficiency, we restrict the input window size to 96.

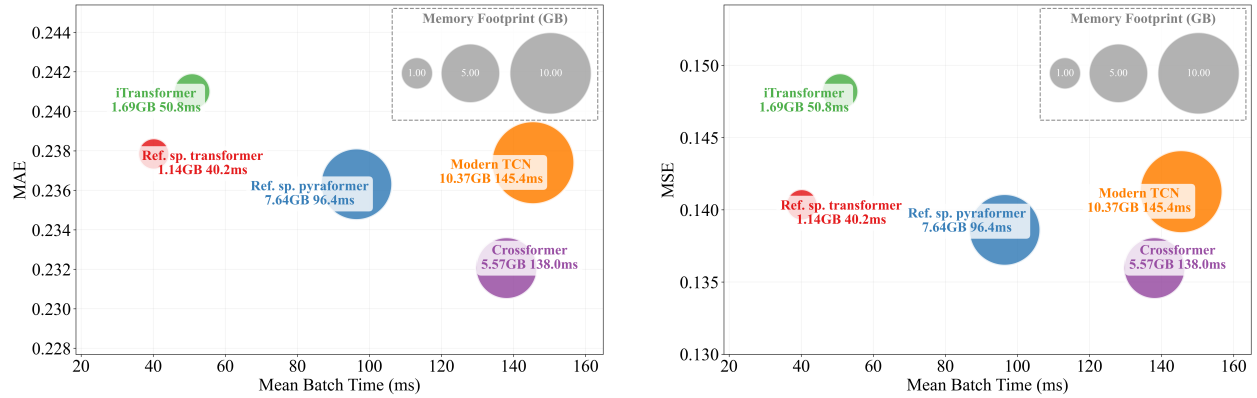


Figure 4: MAE and MSE performance versus mean batch time during training for models *including* spatial processing, for a batch size of 32. Circle size indicates memory consumption.

#### E Implementation details

Our code is implemented in Python [Van Rossum and Drake, 2009], with the use of the following libraries:

- PyTorch [Paszke et al., 2019];
- PyTorch Geometric [Fey and Lenssen, 2019];
- Torch Spatiotemporal [Cini and Marisca, 2022];
- Scikit-learn [Pedregosa et al., 2011];
- PyTorch Lightning [Falcon and The PyTorch Lightning team, 2019];
- Hydra [Yadan, 2019];
- Numpy [Harris et al., 2020].

#### F Forecasting model cards

In Tab. 19, we report an example of the usage of the newly introduced forecasting model cards for PatchTST.

Table 11: Results (MSE and MAE) for multiple horizons. Best mean results are in **bold**, second best are underlined.

Model	H	Electricity		Weather		Traffic		Solar	
		MSE	MAE	MSE	MAE	MSE	MAE	MSE	MAE
OLS Global	96	0.140	0.237	0.174	0.234	0.410	0.282	0.222	0.291
	192	0.154	0.250	0.215	0.272	0.423	0.288	0.249	0.309
	336	0.169	0.268	0.260	0.309	0.436	0.295	0.269	0.324
	720	0.204	0.301	0.323	0.361	0.466	0.315	0.271	0.327
OLS Local	96	0.134	0.230	<b>0.144</b>	0.209	0.426	0.298	0.223	0.295
	192	0.149	0.245	<b>0.187</b>	0.254	0.438	0.304	0.251	0.313
	336	0.165	0.263	<b>0.240</b>	0.298	0.452	0.312	0.270	0.327
	720	0.201	0.297	<b>0.316</b>	0.358	0.482	0.330	0.272	0.331
R. MLP	96	$0.129 \pm 0.000$	$0.225 \pm 0.000$	$0.148 \pm 0.001$	$0.198 \pm 0.000$	$0.376 \pm 0.000$	$0.253 \pm 0.001$	$0.194 \pm 0.003$	$0.239 \pm 0.002$
	192	$0.149 \pm 0.000$	$0.245 \pm 0.001$	$0.191 \pm 0.001$	$0.241 \pm 0.000$	$0.403 \pm 0.001$	$0.270 \pm 0.001$	$0.227 \pm 0.001$	$0.262 \pm 0.001$
	336	$0.166 \pm 0.000$	$0.262 \pm 0.000$	$0.245 \pm 0.001$	$0.281 \pm 0.001$	$0.417 \pm 0.001$	$0.277 \pm 0.001$	$0.249 \pm 0.001$	$0.277 \pm 0.002$
	720	$0.205 \pm 0.000$	$0.296 \pm 0.000$	$0.324 \pm 0.002$	$0.338 \pm 0.001$	$0.456 \pm 0.001$	$0.295 \pm 0.001$	$0.254 \pm 0.000$	$0.279 \pm 0.001$
R. RNN	96	<u><math>0.127 \pm 0.001</math></u>	<u><math>0.221 \pm 0.000</math></u>	$0.148 \pm 0.000$	$0.199 \pm 0.001$	$0.362 \pm 0.002$	$0.248 \pm 0.001$	$0.192 \pm 0.002$	<b><math>0.236 \pm 0.001</math></b>
	192	<u><math>0.167 \pm 0.001</math></u>	<u><math>0.267 \pm 0.001</math></u>	<u><math>0.190 \pm 0.001</math></u>	$0.244 \pm 0.001$	$0.411 \pm 0.005$	$0.282 \pm 0.005$	$0.230 \pm 0.003$	$0.270 \pm 0.002$
	336	<u><math>0.186 \pm 0.001</math></u>	<u><math>0.287 \pm 0.001</math></u>	<u><math>0.244 \pm 0.001</math></u>	$0.286 \pm 0.001$	$0.423 \pm 0.019$	$0.285 \pm 0.005$	$0.251 \pm 0.007$	$0.284 \pm 0.007$
	720	$0.225 \pm 0.002$	$0.323 \pm 0.001$	$0.324 \pm 0.003$	$0.342 \pm 0.003$	$0.497 \pm 0.040$	$0.297 \pm 0.001$	$0.249 \pm 0.005$	$0.281 \pm 0.005$
R. TCN	96	$0.130 \pm 0.000$	$0.224 \pm 0.000$	$0.148 \pm 0.000$	$0.200 \pm 0.001$	$0.364 \pm 0.003$	$0.253 \pm 0.002$	$0.193 \pm 0.004$	$0.243 \pm 0.005$
	192	$0.148 \pm 0.000$	$0.240 \pm 0.000$	$0.195 \pm 0.001$	$0.246 \pm 0.000$	<u><math>0.382 \pm 0.001</math></u>	$0.261 \pm 0.001$	<b><math>0.221 \pm 0.002</math></b>	<b><math>0.253 \pm 0.002</math></b>
	336	$0.165 \pm 0.001$	<u><math>0.258 \pm 0.001</math></u>	$0.252 \pm 0.002$	$0.289 \pm 0.001$	$0.397 \pm 0.002$	$0.274 \pm 0.005$	$0.249 \pm 0.005$	<b><math>0.271 \pm 0.005</math></b>
	720	$0.202 \pm 0.002$	<u><math>0.292 \pm 0.001</math></u>	$0.329 \pm 0.001$	$0.342 \pm 0.001$	<b><math>0.434 \pm 0.001</math></b>	<u><math>0.291 \pm 0.005</math></u>	<u><math>0.246 \pm 0.004</math></u>	<u><math>0.273 \pm 0.003</math></u>
R. Transf.	96	$0.129 \pm 0.001$	$0.222 \pm 0.001$	$0.149 \pm 0.001$	$0.203 \pm 0.002$	<u><math>0.362 \pm 0.003</math></u>	$0.249 \pm 0.002$	$0.203 \pm 0.006$	$0.245 \pm 0.002$
	192	<u><math>0.146 \pm 0.000</math></u>	<u><math>0.238 \pm 0.000</math></u>	$0.198 \pm 0.001$	$0.250 \pm 0.002$	<b><math>0.374 \pm 0.001</math></b>	<b><math>0.255 \pm 0.001</math></b>	<u><math>0.224 \pm 0.001</math></u>	$0.260 \pm 0.001$
	336	<u><math>0.164 \pm 0.001</math></u>	<u><math>0.258 \pm 0.001</math></u>	$0.248 \pm 0.001$	$0.289 \pm 0.002$	<b><math>0.393 \pm 0.002</math></b>	$0.271 \pm 0.007$	<u><math>0.245 \pm 0.004</math></u>	<b><math>0.271 \pm 0.003</math></b>
	720	$0.202 \pm 0.003$	$0.294 \pm 0.002$	$0.330 \pm 0.010$	$0.344 \pm 0.006$	<b><math>0.434 \pm 0.004</math></b>	$0.294 \pm 0.008$	$0.248 \pm 0.004$	$0.277 \pm 0.004$
R. Pyraf.	96	$0.129 \pm 0.001$	$0.224 \pm 0.001$	$0.148 \pm 0.001$	$0.199 \pm 0.001$	$0.365 \pm 0.002$	$0.251 \pm 0.003$	<b><math>0.189 \pm 0.003</math></b>	<b><math>0.236 \pm 0.004</math></b>
	192	$0.147 \pm 0.001$	$0.240 \pm 0.000$	$0.196 \pm 0.003$	$0.246 \pm 0.002$	$0.384 \pm 0.003$	$0.262 \pm 0.004$	<u><math>0.224 \pm 0.001</math></u>	$0.256 \pm 0.001$
	336	<u><math>0.164 \pm 0.001</math></u>	<u><math>0.258 \pm 0.000</math></u>	$0.248 \pm 0.003$	$0.287 \pm 0.003$	$0.397 \pm 0.002$	<u><math>0.269 \pm 0.002</math></u>	<b><math>0.244 \pm 0.001</math></b>	<b><math>0.271 \pm 0.002</math></b>
	720	<u><math>0.200 \pm 0.000</math></u>	$0.293 \pm 0.000$	$0.328 \pm 0.003$	$0.344 \pm 0.002$	<b><math>0.434 \pm 0.002</math></b>	$0.297 \pm 0.003$	$0.248 \pm 0.002$	<b><math>0.272 \pm 0.001</math></b>
TimeMixer	96	$0.129 \pm 0.001$	$0.224 \pm 0.000$	$0.147 \pm 0.001$	<u><math>0.197 \pm 0.000</math></u>	$0.373 \pm 0.002$	$0.271 \pm 0.003$	$0.199 \pm 0.001$	$0.245 \pm 0.000$
	192	$0.147 \pm 0.001$	$0.241 \pm 0.000$	$0.191 \pm 0.000$	<b><math>0.239 \pm 0.000</math></b>	$0.396 \pm 0.001$	$0.283 \pm 0.001$	$0.230 \pm 0.003$	$0.268 \pm 0.003$
	336	$0.166 \pm 0.001$	$0.260 \pm 0.001$	<u><math>0.244 \pm 0.002</math></u>	<u><math>0.281 \pm 0.002</math></u>	$0.416 \pm 0.001$	$0.297 \pm 0.001$	<b><math>0.244 \pm 0.002</math></b>	$0.280 \pm 0.000$
	720	$0.206 \pm 0.003$	$0.297 \pm 0.003$	<u><math>0.321 \pm 0.003</math></u>	<u><math>0.334 \pm 0.003</math></u>	$0.450 \pm 0.006$	$0.318 \pm 0.003$	<b><math>0.245 \pm 0.004</math></b>	$0.280 \pm 0.001$
PatchTST	96	<b><math>0.125 \pm 0.000</math></b>	<b><math>0.218 \pm 0.000</math></b>	$0.148 \pm 0.001$	<b><math>0.195 \pm 0.001</math></b>	<b><math>0.345 \pm 0.000</math></b>	<b><math>0.234 \pm 0.000</math></b>	$0.197 \pm 0.001$	$0.244 \pm 0.004$
	192	<b><math>0.143 \pm 0.000</math></b>	<b><math>0.236 \pm 0.000</math></b>	$0.194 \pm 0.000$	<b><math>0.239 \pm 0.001</math></b>	$0.384 \pm 0.001$	<u><math>0.258 \pm 0.001</math></u>	$0.227 \pm 0.002$	$0.260 \pm 0.002$
	336	<b><math>0.160 \pm 0.000</math></b>	<b><math>0.254 \pm 0.000</math></b>	$0.247 \pm 0.000$	<b><math>0.279 \pm 0.001</math></b>	<u><math>0.396 \pm 0.001</math></u>	<b><math>0.264 \pm 0.000</math></b>	$0.249 \pm 0.001$	<u><math>0.273 \pm 0.002</math></u>
	720	<b><math>0.197 \pm 0.001</math></b>	<b><math>0.288 \pm 0.001</math></b>	$0.322 \pm 0.002$	<b><math>0.333 \pm 0.001</math></b>	<u><math>0.435 \pm 0.001</math></u>	<b><math>0.286 \pm 0.000</math></b>	$0.247 \pm 0.001$	<u><math>0.273 \pm 0.002</math></u>
DLinear	96	$0.140 \pm 0.000$	$0.237 \pm 0.000$	$0.173 \pm 0.000$	$0.232 \pm 0.001$	$0.407 \pm 0.000$	$0.283 \pm 0.000$	$0.246 \pm 0.001$	$0.331 \pm 0.000$
	192	$0.154 \pm 0.000$	$0.250 \pm 0.001$	$0.216 \pm 0.001$	$0.274 \pm 0.003$	$0.421 \pm 0.000$	$0.290 \pm 0.000$	$0.267 \pm 0.001$	$0.342 \pm 0.000$
	336	$0.169 \pm 0.000$	$0.268 \pm 0.000$	$0.265 \pm 0.002$	$0.318 \pm 0.003$	$0.433 \pm 0.000$	$0.296 \pm 0.000$	$0.289 \pm 0.001$	$0.353 \pm 0.000$
	720	$0.203 \pm 0.000$	$0.300 \pm 0.000$	$0.331 \pm 0.002$	$0.373 \pm 0.003$	$0.461 \pm 0.000$	$0.314 \pm 0.000$	$0.294 \pm 0.001$	$0.355 \pm 0.000$

Table 12: Performance and resource utilization of the models selected in 4.3 on the Electricity dataset. Best performance is shown in **bold**, second best is underlined.

Model	Horizon	Batch Time (ms)	Batches per Second	GPU Mem. (MB)	CUDA Time (ms)
MLP	96	<u>27.6<math>\pm</math>1.4</u>	<u>36.3<math>\pm</math>1.2</u>	628.0	<u>20.3</u>
	192	<u>27.6<math>\pm</math>1.4</u>	<u>36.3<math>\pm</math>1.2</u>	628.0	<u>27.1</u>
	336	<u>27.6<math>\pm</math>1.4</u>	<u>36.3<math>\pm</math>1.2</u>	653.2	<u>26.3</u>
	720	<u>27.6<math>\pm</math>1.4</u>	<u>36.3<math>\pm</math>1.2</u>	705.6	<u>31.8</u>
RNN	96	36.7 $\pm$ 0.9	28.2 $\pm$ 0.6	3635.2	235.6
	192	37.3 $\pm$ 2.9	27.8 $\pm$ 1.8	3643.5	243.0
	336	37.3 $\pm$ 2.9	27.8 $\pm$ 1.8	3854.3	246.7
	720	37.3 $\pm$ 2.9	27.8 $\pm$ 1.8	3860.6	258.5
TCN	96	29.9 $\pm$ 1.4	33.5 $\pm$ 1.1	1217.3	62.0
	192	29.9 $\pm$ 1.4	33.5 $\pm$ 1.1	1217.3	82.0
	336	29.9 $\pm$ 1.4	33.5 $\pm$ 1.1	1219.4	85.1
	720	29.9 $\pm$ 1.4	33.5 $\pm$ 1.1	1240.4	87.8
Transf.	96	36.7 $\pm$ 1.3	27.3 $\pm$ 0.7	1942.9	119.3
	192	36.7 $\pm$ 1.3	27.3 $\pm$ 0.7	1961.7	144.0
	336	36.7 $\pm$ 1.3	27.3 $\pm$ 0.7	1959.7	148.1
	720	36.7 $\pm$ 1.3	27.3 $\pm$ 0.7	1976.4	164.7
Pyraf.	96	41.7 $\pm$ 0.8	24.0 $\pm$ 0.4	2559.4	189.9
	192	41.7 $\pm$ 0.8	24.0 $\pm$ 0.4	2561.5	191.9
	336	41.7 $\pm$ 0.8	24.0 $\pm$ 0.4	2563.6	192.8
	720	41.7 $\pm$ 0.8	24.0 $\pm$ 0.4	2567.8	198.7
DLinear	96	<b>18.9<math>\pm</math>1.1</b>	<b>52.9<math>\pm</math>1.7</b>	<b>615.5</b>	<b>10.7</b>
	192	<b>18.9<math>\pm</math>1.1</b>	<b>52.9<math>\pm</math>1.7</b>	<b>615.5</b>	<b>17.2</b>
	336	<b>18.9<math>\pm</math>1.1</b>	<b>52.9<math>\pm</math>1.7</b>	<b>638.5</b>	<b>19.1</b>
	720	<b>18.9<math>\pm</math>1.1</b>	<b>52.9<math>\pm</math>1.7</b>	<b>699.4</b>	<b>22.5</b>
PatchTST	96	34.3 $\pm$ 0.5	29.1 $\pm$ 0.4	1445.9	74.9
	192	34.3 $\pm$ 0.5	29.1 $\pm$ 0.4	1443.8	94.6
	336	34.3 $\pm$ 0.5	29.1 $\pm$ 0.4	1443.8	93.6
	720	34.3 $\pm$ 0.5	29.1 $\pm$ 0.4	1462.7	107.7
TimeMixer	96	97.6 $\pm$ 93.5	10.9 $\pm$ 0.7	2301.5	410.4
	192	97.6 $\pm$ 93.5	10.9 $\pm$ 0.7	2303.6	405.1
	336	97.6 $\pm$ 93.5	10.9 $\pm$ 0.7	2311.9	375.9
	720	97.6 $\pm$ 93.5	10.9 $\pm$ 0.7	2450.3	478.8

Table 13: Results (MSE and MAE) across datasets and horizons. Best mean results are in **bold**, second best are underlined. A dash (–) marks experiments beyond our computational budget.

Model	H	Electricity		Weather		Traffic		Solar	
		MSE	MAE	MSE	MAE	MSE	MAE	MSE	MAE
MLP + sp. attn.	96	0.140±0.001	0.238±0.001	0.157±0.000	<u>0.202±0.001</u>	0.435±0.006	0.275±0.001	0.201±0.009	0.246±0.003
	192	0.167±0.002	0.263±0.002	0.206±0.001	<b>0.249±0.001</b>	0.454±0.008	<u>0.286±0.003</u>	0.237±0.003	0.272±0.003
	336	0.182±0.002	0.281±0.002	0.264±0.001	<u>0.292±0.001</u>	0.472±0.007	0.292±0.004	0.266±0.006	0.294±0.005
	720	0.209±0.008	<u>0.305±0.006</u>	0.349±0.001	<u>0.345±0.001</u>	0.523±0.003	0.316±0.003	0.266±0.004	0.304±0.007
Pyraf. + sp. attn.	96	<u>0.139±0.001</u>	<u>0.236±0.001</u>	0.157±0.002	0.204±0.001	<b>0.389±0.002</b>	<u>0.267±0.001</u>	<u>0.188±0.002</u>	0.235±0.003
	192	<u>0.157±0.000</u>	<u>0.254±0.000</u>	0.207±0.001	<u>0.251±0.002</u>	<b>0.410±0.001</b>	<u>0.276±0.002</u>	0.234±0.003	0.270±0.008
	336	<u>0.174±0.002</u>	<u>0.273±0.002</u>	0.267±0.001	0.294±0.002	<b>0.420±0.001</b>	<u>0.283±0.001</u>	0.248±0.001	0.281±0.004
	720	<b>0.194±0.001</b>	<b>0.292±0.001</b>	0.348±0.002	0.347±0.000	<b>0.449±0.002</b>	<u>0.300±0.001</u>	0.249±0.001	0.280±0.002
iTransformer	96	0.148±0.000	0.241±0.000	0.171±0.001	0.210±0.001	<u>0.393±0.001</u>	<b>0.266±0.001</b>	0.208±0.003	0.240±0.006
	192	0.166±0.001	0.259±0.001	0.221±0.001	0.255±0.000	<u>0.424±0.001</u>	<u>0.286±0.001</u>	<u>0.233±0.003</u>	0.257±0.003
	336	0.179±0.002	0.274±0.002	0.276±0.000	0.295±0.000	<u>0.430±0.001</u>	<u>0.289±0.001</u>	<u>0.244±0.000</u>	0.273±0.002
	720	0.218±0.000	0.309±0.001	0.353±0.000	0.346±0.000	<u>0.455±0.001</u>	0.303±0.000	0.255±0.002	0.280±0.001
Crosformer	96	<b>0.136±0.000</b>	<b>0.232±0.001</b>	<b>0.152±0.003</b>	0.222±0.004	0.527±0.002	0.270±0.003	<b>0.184±0.008</b>	<u>0.227±0.006</u>
	192	0.161±0.003	0.257±0.003	<b>0.200±0.007</b>	0.271±0.007	0.541±0.002	<b>0.276±0.002</b>	<b>0.207±0.015</b>	<b>0.246±0.003</b>
	336	0.187±0.007	0.286±0.007	<u>0.263±0.001</u>	0.325±0.003	0.561±0.005	<u>0.289±0.002</u>	<b>0.222±0.016</b>	<b>0.252±0.001</b>
	720	–	–	0.359±0.007	0.389±0.004	–	–	<b>0.214±0.001</b>	<b>0.250±0.004</b>
ModernTCN	96	0.141±0.000	0.237±0.001	<u>0.154±0.001</u>	<b>0.200±0.001</b>	0.445±0.001	0.287±0.001	0.190±0.001	<b>0.222±0.002</b>
	192	<b>0.156±0.001</b>	<b>0.249±0.001</b>	<u>0.201±0.002</u>	0.252±0.002	–	–	0.235±0.001	<u>0.250±0.002</u>
	336	<b>0.172±0.003</b>	<b>0.263±0.001</b>	<b>0.254±0.003</b>	<b>0.291±0.002</b>	–	–	0.258±0.004	<u>0.266±0.003</u>
	720	<u>0.201±0.000</u>	<b>0.292±0.000</b>	<b>0.338±0.005</b>	<b>0.343±0.005</b>	–	–	0.262±0.003	<u>0.277±0.004</u>

Table 14: Ablation study on iTransformer for window=96 across different forecasting horizons. Best mean results are in **bold**.

Dataset	Horizon	With space attention		Without space attention	
		MSE	MAE	MSE	MAE
Electricity	96	<b>0.148±0.000</b>	0.241±0.000	0.149±0.001	<b>0.237±0.001</b>
	192	0.166±0.001	0.259±0.001	<b>0.161±0.000</b>	<b>0.250±0.000</b>
	336	0.179±0.002	0.274±0.002	0.179±0.000	<b>0.268±0.000</b>
	720	<b>0.218±0.000</b>	0.309±0.001	0.219±0.000	<b>0.303±0.000</b>
Weather	96	0.171±0.001	0.210±0.001	0.171±0.000	0.210±0.001
	192	0.221±0.001	0.255±0.000	<b>0.219±0.001</b>	<b>0.253±0.001</b>
	336	0.276±0.000	0.295±0.000	<b>0.275±0.000</b>	<b>0.294±0.000</b>
	720	0.353±0.000	0.346±0.000	<b>0.352±0.001</b>	<b>0.345±0.000</b>
Traffic	96	0.393±0.001	0.266±0.001	<b>0.390±0.001</b>	<b>0.258±0.000</b>
	192	0.424±0.001	0.286±0.001	<b>0.409±0.000</b>	<b>0.268±0.000</b>
	336	0.430±0.001	0.289±0.001	<b>0.423±0.000</b>	<b>0.274±0.000</b>
	720	0.455±0.001	0.303±0.000	<b>0.454±0.000</b>	<b>0.292±0.000</b>
Solar	96	0.208±0.003	0.240±0.006	<b>0.194±0.001</b>	<b>0.230±0.002</b>
	192	0.233±0.003	0.257±0.003	<b>0.226±0.001</b>	0.257±0.003
	336	<b>0.244±0.000</b>	0.273±0.002	0.245±0.003	<b>0.267±0.002</b>
	720	0.255±0.002	0.280±0.001	<b>0.249±0.001</b>	<b>0.271±0.001</b>

Table 15: Ablation study on iTransformer for window=336 across different forecasting horizons. Best mean results are in **bold**.

Dataset	Horizon	With space attention		Without space attention	
		MSE	MAE	MSE	MAE
Electricity	96	0.135 $\pm$ 0.001	0.229 $\pm$ 0.001	<b>0.130<math>\pm</math>0.000</b>	<b>0.223<math>\pm</math>0.000</b>
	192	0.155 $\pm$ 0.001	0.248 $\pm$ 0.001	<b>0.149<math>\pm</math>0.000</b>	<b>0.242<math>\pm</math>0.000</b>
	336	0.172 $\pm$ 0.002	0.267 $\pm$ 0.000	<b>0.166<math>\pm</math>0.000</b>	<b>0.260<math>\pm</math>0.000</b>
	720	<b>0.201<math>\pm</math>0.002</b>	0.294 $\pm$ 0.002	0.205 $\pm$ 0.000	0.294 $\pm$ 0.000
Weather	96	0.159 $\pm$ 0.001	0.207 $\pm$ 0.000	<b>0.153<math>\pm</math>0.000</b>	<b>0.202<math>\pm</math>0.001</b>
	192	0.203 $\pm$ 0.001	0.249 $\pm$ 0.001	<b>0.197<math>\pm</math>0.001</b>	<b>0.245<math>\pm</math>0.002</b>
	336	0.252 $\pm$ 0.002	0.286 $\pm$ 0.000	<b>0.249<math>\pm</math>0.001</b>	<b>0.284<math>\pm</math>0.001</b>
	720	<b>0.326<math>\pm</math>0.003</b>	<b>0.338<math>\pm</math>0.002</b>	0.328 $\pm$ 0.002	0.339 $\pm$ 0.001
Traffic	96	0.363 $\pm$ 0.000	0.257 $\pm$ 0.001	<b>0.359<math>\pm</math>0.001</b>	<b>0.247<math>\pm</math>0.001</b>
	192	0.385 $\pm$ 0.002	0.269 $\pm$ 0.001	<b>0.377<math>\pm</math>0.001</b>	<b>0.256<math>\pm</math>0.001</b>
	336	0.397 $\pm$ 0.002	0.277 $\pm$ 0.001	<b>0.386<math>\pm</math>0.000</b>	<b>0.261<math>\pm</math>0.000</b>
	720	0.423 $\pm$ 0.001	0.291 $\pm$ 0.000	<b>0.420<math>\pm</math>0.001</b>	<b>0.282<math>\pm</math>0.000</b>
Solar	96	0.195 $\pm$ 0.000	0.252 $\pm$ 0.003	<b>0.189<math>\pm</math>0.001</b>	<b>0.232<math>\pm</math>0.001</b>
	192	0.222 $\pm$ 0.004	0.269 $\pm$ 0.001	<b>0.207<math>\pm</math>0.000</b>	<b>0.249<math>\pm</math>0.000</b>
	336	0.230 $\pm$ 0.007	0.276 $\pm$ 0.004	<b>0.214<math>\pm</math>0.000</b>	<b>0.255<math>\pm</math>0.001</b>
	720	0.223 $\pm$ 0.002	0.274 $\pm$ 0.003	<b>0.216<math>\pm</math>0.003</b>	<b>0.258<math>\pm</math>0.002</b>

Table 16: Ablation study on iTransformer for window=720 across different forecasting horizons. Best mean results are in **bold**.

Dataset	Horizon	With space attention		Without space attention	
		MSE	MAE	MSE	MAE
Electricity	96	0.135 $\pm$ 0.002	0.231 $\pm$ 0.001	<b>0.132<math>\pm</math>0.000</b>	<b>0.227<math>\pm</math>0.001</b>
	192	0.157 $\pm$ 0.001	0.252 $\pm$ 0.001	<b>0.151<math>\pm</math>0.001</b>	<b>0.245<math>\pm</math>0.001</b>
	336	0.175 $\pm$ 0.001	0.272 $\pm$ 0.001	<b>0.165<math>\pm</math>0.000</b>	<b>0.263<math>\pm</math>0.000</b>
	720	<b>0.195<math>\pm</math>0.001</b>	<b>0.289<math>\pm</math>0.002</b>	0.201 $\pm$ 0.001	0.294 $\pm$ 0.001
Weather	96	0.155 $\pm$ 0.002	0.208 $\pm$ 0.002	<b>0.149<math>\pm</math>0.000</b>	<b>0.201<math>\pm</math>0.001</b>
	192	0.202 $\pm$ 0.002	0.250 $\pm$ 0.001	<b>0.195<math>\pm</math>0.001</b>	<b>0.247<math>\pm</math>0.002</b>
	336	0.249 $\pm$ 0.002	<b>0.288<math>\pm</math>0.002</b>	0.249 $\pm$ 0.001	0.289 $\pm$ 0.001
	720	0.322 $\pm$ 0.002	0.342 $\pm$ 0.000	<b>0.317<math>\pm</math>0.001</b>	<b>0.337<math>\pm</math>0.001</b>
Traffic	96	<b>0.353<math>\pm</math>0.004</b>	0.256 $\pm$ 0.001	0.357 $\pm$ 0.000	<b>0.251<math>\pm</math>0.000</b>
	192	0.372 $\pm$ 0.002	0.267 $\pm$ 0.000	<b>0.369<math>\pm</math>0.000</b>	<b>0.260<math>\pm</math>0.000</b>
	336	0.388 $\pm$ 0.002	0.276 $\pm$ 0.001	<b>0.383<math>\pm</math>0.001</b>	<b>0.269<math>\pm</math>0.001</b>
	720	<b>0.417<math>\pm</math>0.002</b>	0.290 $\pm$ 0.001	0.420 $\pm$ 0.000	<b>0.287<math>\pm</math>0.000</b>
Solar	96	<b>0.175<math>\pm</math>0.003</b>	0.245 $\pm$ 0.004	0.182 $\pm$ 0.008	<b>0.235<math>\pm</math>0.006</b>
	192	<b>0.197<math>\pm</math>0.001</b>	0.262 $\pm$ 0.002	0.200 $\pm$ 0.003	<b>0.258<math>\pm</math>0.003</b>
	336	0.211 $\pm$ 0.002	0.272 $\pm$ 0.003	<b>0.209<math>\pm</math>0.002</b>	<b>0.262<math>\pm</math>0.002</b>
	720	0.216 $\pm$ 0.001	0.275 $\pm$ 0.003	<b>0.210<math>\pm</math>0.000</b>	<b>0.264<math>\pm</math>0.001</b>

Table 17: Ablation study on iTransformer for horizon=96 across different window lengths. Best mean results are in **bold**.

Dataset	Window	With space attention		Without space attention	
		MSE	MAE	MSE	MAE
Electricity	96	<b>0.148±0.000</b>	0.241±0.000	0.149±0.001	<b>0.237±0.001</b>
	336	0.135±0.001	0.229±0.001	<b>0.130±0.000</b>	<b>0.223±0.000</b>
	720	0.135±0.002	0.231±0.001	<b>0.132±0.000</b>	<b>0.227±0.001</b>
Weather	96	0.171±0.001	0.210±0.001	0.171±0.000	0.210±0.001
	336	0.159±0.001	0.207±0.000	<b>0.153±0.000</b>	<b>0.202±0.001</b>
	720	0.155±0.002	0.208±0.002	<b>0.149±0.000</b>	<b>0.201±0.001</b>
Traffic	96	0.393±0.001	0.266±0.001	<b>0.390±0.001</b>	<b>0.258±0.000</b>
	336	0.363±0.000	0.257±0.001	<b>0.359±0.001</b>	<b>0.247±0.001</b>
	720	<b>0.353±0.004</b>	0.256±0.001	0.357±0.000	<b>0.251±0.000</b>
Solar	96	0.208±0.003	0.240±0.006	<b>0.194±0.001</b>	<b>0.230±0.002</b>
	336	0.195±0.000	0.252±0.003	<b>0.189±0.001</b>	<b>0.232±0.001</b>
	720	<b>0.175±0.003</b>	0.245±0.004	0.182±0.008	<b>0.235±0.006</b>

Table 18: Performance and resource utilization of the models selected in 5 on the Electricity dataset. Best performance is shown in **bold**, second best is underlined.

Model	Horizon	Batch Time (ms)	Batches per Second	GPU Mem. (MB)	CUDA Time (ms)
MLP + sp. att.	96	<b>40.2±1.0</b>	<b>24.9±0.5</b>	<b>1162.8</b>	<b>96.9</b>
	192	<b>40.6±1.3</b>	<b>24.7±0.6</b>	<b>1236.2</b>	<b>123.8</b>
	336	<b>40.6±1.3</b>	<b>24.7±0.6</b>	<b>1215.2</b>	<b>155.4</b>
	720	<b>40.6±1.3</b>	<b>24.7±0.6</b>	<b>1357.8</b>	<b>185.8</b>
Pyraf. + sp. att.	96	96.4±0.4	10.4±0.0	7822.9	783.6
	192	96.4±0.4	10.4±0.0	7908.8	787.3
	336	96.4±0.4	10.4±0.0	7837.5	808.8
	720	96.4±0.4	10.4±0.0	7940.3	861.9
iTransformer	96	<u>50.8±1.3</u>	<u>19.7±0.4</u>	<u>1729.0</u>	<u>217.4</u>
	192	<u>50.7±1.1</u>	<u>19.7±0.4</u>	<u>1630.4</u>	<u>227.9</u>
	336	<u>50.7±1.1</u>	<u>19.7±0.4</u>	<u>1712.2</u>	<u>252.9</u>
	720	<u>50.7±1.1</u>	<u>19.7±0.4</u>	<u>1871.6</u>	<u>317.8</u>
Crossformer	96	138.0±1.0	7.2±0.1	5702.8	912.8
	192	161.9±28.1	6.4±1.0	9412.4	1532.0
	336	161.9±28.1	6.4±1.0	16032.6	2516.0
	720	161.9±28.1	6.4±1.0	39527.4	5589.0
Modern TCN	96	145.4±1.1	6.9±0.0	10620.3	1967.0
	192	147.4±8.8	6.8±0.3	10620.3	1971.0
	336	147.4±8.8	6.8±0.3	10662.2	2005.0
	720	147.4±8.8	6.8±0.3	10857.2	2036.0

Table 19: Example of model cards for PatchTST on the Electricity dataset

<b>FORECASTING MODEL CARD</b>	
<b>Model setting</b>	<ul style="list-style-type: none"> <li>• <i>Window length</i>: fixed lookback window of 336</li> <li>• <i>Transductive or inductive (cold start)</i>: inductive</li> <li>• <i>Masking</i>: not applied/needed</li> </ul>
<b>D1. Model configuration</b>	<ul style="list-style-type: none"> <li>• <i>Global/local/hybrid</i>: global model</li> <li>• <i>Hybrid parameters (non-shared)</i>: not applicable</li> </ul>
<b>D2. Preprocessing and exogenous variables</b>	<ul style="list-style-type: none"> <li>• <i>Scaling</i>: standard normalization (z-score) applied per series and in-batch RevInv normalization</li> <li>• <i>Covariates/exogenous variables</i>: not used</li> </ul>
<b>D3. Temporal processing</b>	<ul style="list-style-type: none"> <li>• <i>Temporal modules</i>: convolutional encoding followed by patching-based Transformer layers</li> <li>• <i>Complexity scaling with steps</i>: the time and space complexity scales quadratically with the number of patches (self-attention)</li> </ul>
<b>D4. Spatial processing</b>	<ul style="list-style-type: none"> <li>• <i>Spatial modules</i>: not applicable</li> <li>• <i>Complexity scaling with nodes</i>: not applicable</li> </ul>